Chapter Two

METHANE SEEP CARBONATES HOST DISTINCT, DIVERSE, AND DYNAMIC MICROBIAL ASSEMBLAGES

David H. Case[1]

in collaboration with,

Alexis L. Pasulka[1], Jeffrey J. Marlow[1], Benjamin M. Grupe[2], Lisa A. Levin[2], and Victoria J. Orphan[1]

[1]Division of Geological and Planetary Sciences, California Institute of Technology, Pasadena, CA, USA

[2]Center for Marine Biodiversity and Conservation, Scripps Institution of Oceanography, University of California – San Diego, La Jolla, CA, USA

*Published in Case et al., 2015. Methane Seep Carbonates Host Distinct, Diverse, and Dynamic Microbial Assemblages. mBio 6 (6), e01348-15.

2.0 ABSTRACT

Marine methane seeps are globally distributed geologic features in which reduced fluids, including methane, are advected upward from the subsurface. As a result of alkalinity generation during sulfate-coupled methane oxidation, authigenic carbonates form slabs, nodules, and extensive pavements. These carbonates shape the landscape within methane seeps, persist long after methane flux is diminished, and in some cases are incorporated into the geologic record. In this study, microbial assemblages from 134 native and experimental samples across 5,500 km, representing a range of habitat substrates (carbonate nodules and slabs, sediment, bottom water, and wood) and seepage conditions (active and low-activity), are analyzed to address two fundamental questions of seep microbial ecology: (1) do carbonates host distinct microbial assemblages, and (2) how sensitive are microbial assemblages to habitat substrate type and temporal shifts in methane seepage flux? Through massively parallel 16S rRNA gene sequencing and statistical analysis, native carbonates are shown to be reservoirs of distinct and highly diverse seep microbial assemblages. Unique coupled transplantation and colonization experiments on the seafloor demonstrate that carbonate-associated microbial assemblages are resilient to seep quiescence and reactive to seep activation over 13 months. Varying rates of response to simulated seep quiescence and activation are observed among similar phylogenies (e.g. *Chloroflexi* OTUs) and similar metabolisms (e.g. putative S-oxidizers), demonstrating the wide range of microbial sensitivity to changes in seepage flux. These results imply that carbonates do not passively record a time-integrated history of seep microorganisms, but rather host distinct, diverse, and dynamic microbial assemblages.

2.1 IMPORTANCE

Since their discovery in 1984, the global distribution and importance of marine methane seeps has become increasingly clear. Much of our understanding of methane seep microorganisms – from metabolisms to community ecology – has stemmed from detailed studies of seep sediments. However, it has become apparent that carbonates represent a volumetrically significant habitat substrate at methane seeps. Through combined *in situ* characterization and incubation experiments this study demonstrates that carbonates host microbial assemblages distinct from and more diverse than other seep habitats. This emphasizes the importance of seep carbonates as biodiversity locales. Furthermore, we demonstrate that carbonate-associated microbial assemblages are well adapted to withstand fluctuations in methane seepage, and we gain novel insight into particular taxa that are responsive (or recalcitrant) to changes in seep conditions.

2.2 INTRODUCTION

Marine methane seeps serve as islands of diverse and dense deep-sea life, with food webs extending from microorganisms to varied megafauna including clams, mussels, and tube worms (Levin 2005; Thurber et al. 2012; Niemann et al. 2013). Distinct habitats associated with methane seeps include sediments, bottom water, loosely consolidated carbonate protoliths (hereafter "nodules"), fully lithified carbonate blocks and pavements (hereafter "carbonates"), and, occasionally, wood. Marine methane seep microbial communities and corresponding geochemistry within sediments have been intensively investigated, and have been found to frequently be dominated by microbial taxa performing anaerobic oxidation of methane (AOM), notably anaerobic methane-oxidizing archaea (ANME) and deltaproteobacterial sulfate-reducing bacteria (SRB; Hinrichs et al. 1999; Orphan et al. 2001; Pop Ristova et al. 2015). More broadly, seep sediments are biologically diverse locales that host microorganisms spanning many phyla, and are often rich in Epsilonproteobacteria and Gammaproteobacteria in addition to the canonical AOM-associated taxa (Nunoura et al. 2012; Ruff et al. 2013; Marlow et al. 2014b; Pop Ristova et al. 2015). A distinct "seep microbiome", rich in Deltaproteobacteria, Methanomicrobia, and Candidate Divisions Hyd24-12 and JS1, is apparent when comparing seep sediment- and nodule-associated microbial assemblages to other marine environments (Ruff et al. 2015).

Authigenic carbonates, which are believed to form as a result of increased alkalinity associated with AOM metabolism, constitute the most pervasive solid habitat substrate at methane seeps, but are historically less well sampled than sediments. Carbonates are known to host lipid (Thiel et al. 2001; Stadnitskaia et al. 2005) and ribosomal DNA (Stadnitskaia et al. 2005; Heijs et al. 2006; Marlow et al. 2014b) biomarkers, as well as record carbon isotopic compositions reflective of microbial AOM processes (Greinert et al. 2001; Gieskes et al. 2005). Seep carbonates have recently been shown to host viable autoendolithic (organisms whose

metabolism induces self-entombing mineral formation) Archaea and Bacteria capable of methane oxidation (Marlow et al. 2014a; 2015), as well a metazoan communities (Levin et al. 2015). Carbonates themselves occur in a variety of sizes, morphologies, and mineralogies. These include mm- to cm-scale poorly consolidated precipitates, termed "nodules" or "concretions", occurring within seep sediments (Chen et al. 2006; Watanabe et al. 2008; Mason et al. 2015). Seep-associated carbonates are also frequently found exposed at the seafloor in cm- to 10s of m-sized isolated blocks and continuous pavements (Hovland et al. 1987; Naehr et al. 2007), often extending both laterally and vertically from the site of contemporary methane seepage (Teichert et al. 2005; Sahling et al. 2008). Observations of carbonates at sites lacking contemporary seepage provide evidence that carbonates can outlive seepage processes on the seafloor, supported by the recovery of demonstrably seep-associated carbonates from geologic outcrops as old as 300 million years (Birgel et al. 2008). Diversity relationships between microbial assemblages associated with seep sediments, nodules, and carbonates have just recently begun to be explored (Marlow et al. 2014b; Mason et al. 2015).

Seepage flux can increase and decrease, as well as shift spatially, on the scale of days (Tryon et al. 2002) to weeks (Tryon et al. 1999) to centuries (Bekins and Dreiss 1992; Tryon et al. 2002). Microbial assemblages presumably adapt to spatial and temporal changes in seepage flux, but the extent and rate of response *in situ* remains uncharacterized. Contemporary seepage activity is often defined categorically based on the presence or absence of diagnostic seafloor chemosynthetic communities within methane seeps. "Active" sites are defined, in this study and elsewhere (Tryon et al. 2002; Orphan et al. 2004; Boetius and Suess 2004; Levin et al. 2015), as hosting sulfur-oxidizing bacterial mats, clam beds, dense snail colonies, and/or methane ebullition, while "low-activity" areas lack those diagnostic indicators of contemporary seepage. Notably, low-activity sites are often within $<10^2$ meters from active sites, frequently host carbonates, and can still exhibit microbial activity, including AOM, at reduced rates (Marlow et al. 2014a). Diversity surveys using conventional cloning and sequencing have shown that seep-

associated archaeal assemblages, of which only a fraction of the taxa were ANME subgroups, differed based on local seepage activity. The same trend was not apparent in bacterial assemblage composition, which instead was more influenced by habitat substrate (sediment vs nodule vs carbonate; Marlow et al. 2014b). Lipid biomarker profiles from seep sediment and microbial mat samples have been shown to be differentiated partially by sulfate reduction rate, which is likely in turn correlated with seep activity (Rossel et al. 2011). Off-seep sites host microbial assemblages that are distinct from both active and low-activity sites, further indicating the existence of a "seep microbiome" (Marlow et al. 2014b; Pop Ristova et al. 2015; Ruff et al. 2015).

Here a combined comparative and experimental *in situ* approach is applied to characterize the relationship between seep microbial assemblages, habitat substrata (carbonate vs sediment vs nodule vs bottom water vs wood), and varying seep activity (active vs low-activity stations). By coupling a massive sampling effort of native, unperturbed seep carbonates to *in situ* transplantation and colonization experiments, we can leverage these compatible datasets to address two fundamental microbial ecology questions: (1) do seep carbonates host distinct microbial assemblages, and (2) how sensitive are microbial assemblages to habitat substrate type and availability and temporal shifts in methane seepage flux?

2.3 MATERIALS AND METHODS

2.3.1 SAMPLE COLLECTION AND DEPLOYMENT OF EXPERIMENTS

The majority of samples in this study (114 out of 134; Table S1), including all transplantation and colonization treatments (see below), are from an extensively-studied natural laboratory of methane seepage: namely, the Northern and Southern promontories of Hydrate Ridge ("HR"), on the Cascadia margin, Oregon, USA (HR-North: 44˚40'N, 125˚6'W, ~600 meters below sea level [mbsl], HR-South; 44˚34'N, 125˚9'W, ~800 mbsl, Fig. S1A-B, D-H; Suess

et al. 1985; Boetius et al. 2000; Sahling et al. 2002; Boetius and Suess 2004; Levin et al. 2010; Guilini et al. 2012). Active and low-activity stations were identified by presence (or absence) of benthic chemosynthetic communities throughout HR and given sequential names for experimental purposes (Stations spaced 10^1-10^4 meters apart on the seafloor, see Fig. S1D-E, Table S1). Our active and low-activity station designations were confirmed by pore water sulfide concentrations from 0-3 centimeter-below-seafloor horizons of sediment cores collected within active stations (1-14 mM range, 6mM average, n=9) and low-activity stations (0-0.9 mM range, 0.2 mM average, n=5; more details in Supplemental Text). 110 out of 114 HR samples, including carbonates, sediments, nodules, bottom water, and woods, were collected from these stations, with four additional carbonate samples obtained from a seep promontory approximately 20 km SSE of HR ("Southeast Knoll"; 44˚ 27.0'N, 125˚ 7.8'W, ~620 mbsl). Of the remaining 20 samples in this study, 10 carbonates were collected from seeps off the Costa Rica coast: Mound 11, Mound 12, Quepos Mound, and Jaco Scarp (Fig. S1C; Sahling et al. 2008; Levin et al. 2012; Dekas et al. 2014). As a point of comparison to sediments and nodules collected at HR, we also included ten sediment and nodule samples from Eel River Basin (ERB; 40˚48.7'N, 124˚36.7'W, 517 mbsl; Levin et al. 2003; Orphan et al. 2004). Recently published sequencing data from 18 sediment and nodule samples (13% of our 134-sample dataset) provide valuable context for this study regarding habitat substrate and are denoted in Table S1 (Mason et al. 2015).

Among all the collected samples, 82 out of 134 represent native, unperturbed microbial assemblages associated with a variety of habitat substrates ($n_{carbonate}$=57; n_{nodule}=10; $n_{bottom\ water}$=2; $n_{sediment}$=13) and seep activity levels (n_{active}=52, $n_{low\text{-}activity}$=28, $n_{off\ seep}$=2). Samples were collected in 2006, 2009, 2010, and 2011 during R/V Atlantis cruises AT15-11, AT15-44, AT15-68, and AT18-10, respectively. Upon shipboard retrieval, subsamples were immediately frozen at -80˚C and transferred to an onshore lab for downstream processing. Mineralogy of carbonate samples was examined by powder X-ray diffraction (see Supplemental Text).

Six transplanted carbonate and 46 introduced carbonate and wood (n_{carb}=20, n_{wood}=26) samples represent microbial assemblages after 13 months of incubation on the seafloor. Transplantation experiments were conducted using DSV Alvin in August 2010 by moving seafloor carbonates at HR-North from active to low-activity stations (n=4) and vice versa (n=2), followed by collection and freezing in September 2011 using ROV Jason II. Colonization experiments were conducted with fir and pine woods (n=26) and autoclaved, aseptically stored calcite and dolomite seep carbonates (n=20) deposited at selected seafloor stations, including those of the transplantation experiments, in August 2010 (AT15-68) and recovered in September 2011 (AT18-10). More methodological details regarding the transplantation and colonization experiments can be found in the Supplemental Text.

2.3.2 GENOMIC DNA EXTRACTION AND 16S rRNA GENE SEQUENCING AND PROCESSING

Onshore, the carbonates, sediments, and nodules were separately ground into powder with a sterile porcelain mortar and pestle. The nodules, which were only loosely consolidated and thus could have contained sediment-phase contamination, were pre-processed in order to thoroughly remove sediment as previously described (Mason et al. 2015), with the exception of nodule #5118N (Table S1). Genomic DNA was extracted following the general procedure of the MoBio PowerSoil kit (MoBio, St. Louis, MO, see Orphan et al. 2001 for variations from default protocol), using ~400 mg powder. For wood samples, a sterile razor blade was used to collect shavings from the exterior, avoiding the bark and any observed animals (e.g., shipworms) whenever possible. DNA from wood samples was extracted using the MoBio PowerPlantPro kit's recommended protocol with 40 µL of Phenolic Separation Solution and ~70 mg wood shavings. Bottom water samples from nearby station HR-9 (Fig. S1) were collected on a 0.2 µm filter and

extracted by phenol-chloroform followed by CsCl density gradient centrifugation (Tavormina et al. 2010).

Preparation for sequencing of the V4 region of the 16S rRNA gene was performed with universal primers according to the Earth Microbiome Project (EMP, "iTag" sequencing; Gilbert et al. 2011) recommended protocol (Caporaso et al. 2011; 2012), with minor modifications as previously described (Mason et al. 2015). Raw sequences were generated on an Illumina MiSeq platform at Laragen, Inc. (Los Angeles, CA) and are available in the Sequence Read Archive under accession numbers SRP055767 and SRP049675. In-house data processing was completed in QIIME1.8.0 and included joining paired ends, quality trimming, chimera checking, 97% OTU clustering, singleton removal, PCR contaminant removal, 0.01% relative abundance threshold removal, and rarefaction to 16,051 sequences per sample (Supplemental Text). Taxonomic assignments were generated according to an appended version of the Silva 115 database (details in Mason et al. 2015).

2.3.3 DIVERSITY ANALYSES

Alpha diversity calculations (Shannon Index (H'), Observed OTUs, and Chao1) were carried out in QIIME1.8.0 (alpha_diversity.py). Non-metric multidimensional scaling (NMDS) analyses were carried out in the R environment (R Core Team 2014) after applying a square root transformation to the relative abundance data. For all Analysis of Similarity (ANOSIM) tests, p-values of <0.05 were considered significant. R values are only reported in the text for tests which yielded significant results. Examples of the R commands, including options used, are given in the Supplemental Text. Distance-based Linear Modeling (distLM) was applied with Primer-E software to complement the ANOSIM analysis (Clarke and Warwick 2001). The Similarity Percentage (SIMPER) test was applied in R to identify specific OTUs which demonstrate different relative abundances between sample groups; key OTUs were selected for presentation

and usually represented the majority of sequences associated with each taxonomy (Fig. 3; Fig. 5; Table S3).

2.4 RESULTS AND DISCUSSION

2.4.1 CARBONATES HOST DISTINCT AND DIVERSE SEEP MICROBIAL ASSEMBLAGES

Ordination of the sample set reveals the microbial assemblages to be most strongly differentiated by habitat substrate (i.e. carbonate, sediments and nodules, bottom water; Fig. 1A; $R=0.49$; $p<0.001$; all ANOSIM results presented in Table S2). Habitat substrate is also the most significant factor associated with microbial assemblages as determined by distLM, accounting for 25% of the inter-sample variability. Furthermore, carbonates exhibit higher OTU richness than the other substrates included in this study (Fig. 2A; Chao1 estimates are given in the main text, raw OTU rarefactions are given in Fig. S2). These trends are also observed in the macrofauna recovered from seep carbonates (Levin et al. 2015), confirming carbonates host diverse benthic life across multiple trophic levels. Overall microbial assemblages of sediments and nodules are not statistically differentiable as determined from ANOSIM tests, indicating that sediment-hosted nodules and exhumed seafloor carbonates behave as separate, distinct habitat substrates for microbial habitation (Fig. 1A, Table S2). Sediments, nodules, and carbonates have recently been shown to host different bacterial, but not archaeal, assemblages in 16S clone library surveys (Marlow et al. 2014b), while recent examination of a subset of our iTag data demonstrated similar microbial communities inhabiting nodules and adjacent sediments, especially in active seep settings (Mason et al. 2015).

Examination the top thirty most abundant OTUs in our dataset reveals a variety of Archaea and Bacteria composing the samples (Fig. 3A), including taxonomies common to

methane seep settings (e.g., ANME subgroups and Deltaproteobacteria). The higher relative abundance of ANME-1 in sediments and nodules as compared to carbonates is in agreement with previous clone library observations at Hydrate Ridge, while the recovery of epsilonproteobacterial sequences from sediments, nodules, and carbonates is in contrast to previous findings in which they were almost exclusively recovered from sediments (Fig. 3A; Marlow et al. 2014b). Data from sequencing of mock communities suggests a slight bias for ANME-1 and stronger bias against the recovery of ANME-2 sequences by the modified EMP protocol (Trembath-Reichert et al., 2016). Thus, we note the relative abundance of these groups may in reality be slightly lower (ANME-1) or higher (ANME-2) than recovered in our iTag dataset. However, the inter-substrate trends, which are similar for ANME-1 and ANME-2, should be unaffected. Abundance patterns of ANME and other taxa are discussed in detail in the sections below, in the context of results from our experimental manipulations.

Inter-substrate differences in microbial assemblage are the cumulative result of contributions from many OTUs, with no single OTU accounting for more than 2% of the total inter-substrate differences. Nonetheless, several OTUs can be identified which are strongly associated with one habitat type (Fig. 3B). Notably, taxa previously identified as diagnostic of the "seep microbiome" (i.e., JS1 archaea and Deltaproteobacteria; Ruff et al. 2015) are observed in our dataset to be characteristic of sediments and nodules, but not carbonate habitats (Fig. 3B). In determining the "seep microbiome," Ruff et al., 2015 examined methane seep sediments and nodules exclusively; our data thus corroborate their results, but also further demonstrate that seep carbonates host distinct microbial assemblages. Carbonates, to the exclusion of other habitat substrates, are observed to host an OTU associated with the gammaproteobacterial JTB255 Marine Benthic Group (Fig. 3B). The physiology of this group remains undetermined, though uncultured members have been recovered from a variety of marine sediments (Bowman and McCuaig 2003; Schauer et al. 2010), including methane seeps (Li et al. 1999). OTUs associated with the deltaproteobacterial SAR324 clade and thaumarchaeal Marine Group 1 are particularly

abundant in the bottom water samples (Fig. 3B), although we note that a separate thaumarchaeal Marine Group 1 OTU is more abundant on carbonates than on other substrates (Fig. 3A). This exemplifies the potential for OTUs of similar phylogeny to be differentially distributed in the environment.

Shannon diversity (H'), which measures evenness in addition to richness, is higher in the carbonates than either the sediments/nodules or the bottom waters (Fig. S2D). Carbonate-associated assemblages may exhibit distinct microbial molecular signatures due to either geochemical (i.e., preferential adsorption of metabolites to the carbonate matrix; Ijiri et al. 2009), physical (i.e., a site for microbial biofilm attachment), or historic (i.e., formation within or above the sediment column; Blumenberg et al. 2015) factors. Examination of the OTU overlap among native habitat substrates (Fig. 4A) demonstrates that carbonates share more OTUs with sediments and nodules than bottom waters, supporting the hypothesis of formation within the sediments, followed by subsequent exhumation and exposure at the seafloor (Gieskes et al. 2005; Blumenberg et al. 2015). However, bottom waters share more OTUs with carbonates than sediments or nodules, revealing that a subset of bottom water microorganisms do passively or actively inhabit carbonates exposed at the seafloor (Fig. 4A).

Close overlap in assemblage composition is observed between some of the carbonates (~10 of 57, all from active seep stations) and sediments/nodules (Fig. 1A, c.f. 10 carbonates highlighted in Fig. S3A). It is possible that carbonate samples hosting microbial assemblages similar to sediments/nodules may have contained excess sediment entrained in the rock matrix upon recovery (c.f. Blumenberg et al. 2015); alternatively, nodules in the overlapping regions may have been sufficiently lithified to begin hosting "carbonate-like" microbial assemblages (e.g., nodule #C2693 in Fig. 1A), though this does not necessarily explain similarity of some sediment samples. The compositional overlap between ~10 active-station carbonate assemblages and sediment/nodule assemblages is not derived from geographic proximity, as the sediments/nodules from HR do not exclusively plot in close proximity to the carbonate samples, which are

dominantly from HR (Fig. S3A). Nor are the overlapping carbonates unified by seafloor station, mineralogy, or collection year.

2.4.2 DEMONSTRATION OF MICROBIAL VARIABILITY WITHIN SEEP CARBONATES

The high total OTU richness of carbonates (Fig. 2A), combined with OTU overlap between carbonates and other substrates (Fig. 4A) could indicate that carbonates represent a passive repository of preserved and extant microorganisms. We test this possibility by first examining in detail, in this section, the native carbonate samples (n=57), which allows inference of the environmental indicators associated with differences between carbonate-hosted microbial assemblages. In the following sections, we then couple these interpretations to the *in situ* transplantation (n=6) and colonization ($n_{carbonate}$=20; n_{wood}=26) experiments, respectively.

On their own, native carbonate-associated microbial assemblages demonstrate clear differentiation according to seep activity (R=0.45; p<0.001; Fig. 1B; Table S2), mineralogy (R=0.44; p<0.001; Fig. S4; Table S2), and seafloor station ($R_{active\ stations}$=0.31, $p_{active\ stations}$=0.002; $R_{low\text{-}activity\ stations}$=0.27, $p_{low\text{-}activity\ stations}$=0.037; Table S2). The similar parsing of native carbonate-hosted assemblages by seep activity and mineralogy is partially explained by our observation of a qualitative relationship between seep activity and carbonate mineralogy, with a higher proportion of aragonite-bearing carbonates recovered from low-activity stations (see Supplemental Text and Fig. S4). This suggests seep activity and carbonate mineralogy are not independent environmental factors in our dataset. The biogeographic differences between stations (~10^2-10^4 m) are in agreement with previous observations of within-seep microbial and geochemical heterogeneity (Treude et al. 2003; Pop Ristova et al. 2015) and recent findings that sediment-associated microorganisms in seeps exhibit "global dispersion and local diversification" (Ruff et al. 2015). A distance-decay curve demonstrated that if a biogeographic effect on microbial similarity exists

over a 10^5-10^6-m scale, it is aliased by other environmental factors (Fig. S5). We frame our further discussion in terms of seep activity because it is strongly associated with differences between carbonate-hosted assemblages and, importantly, our sample collection and *in situ* transplantation and colonization experiments were explicitly performed in order to test biological variability as a function of seep station activity. However, we emphasize that seep activity is a qualitative environmental indicator that may be correlated with other environmental factors, such as carbonate mineralogy.

With regard to standard ecological metrics of OTU richness and evenness (Fig. 2B, Fig. S2B), seep activity does not differentiate the native carbonate-associated microbial assemblages. This indicates that while carbonates at low-activity stations host distinct assemblages, they are not less diverse than microbial assemblages from carbonates at active stations. Active-station carbonates are particularly rich in OTUs associated with putative sulfur-oxidizing organisms belonging to the epsilonproteobacterial and gammaproteobacterial families Helicobacteraceae and Thiotrichaceae, respectively, as compared to carbonates from low-activity stations (Fig. 5 and Table S3). These organisms are likely supported by high sulfide concentrations produced by sulfate-coupled AOM at active seep stations. Among seep sediments in the Mediterranean Sea, epsilonproteobacterial Helicobacteraceae were found to be an indicator taxa for seepage (Pop Ristova et al. 2015), which our data corroborate. Data from hydrothermal vent systems also exhibit clear differences in abundance of putative sulfur-oxidizing Epsilonproteobacteria between active and low-activity (or inactive) sites, with increased abundance at active vent sites where delivery of reduced fluids is high (Sylvan et al. 2012b). Furthermore, Epsilonproteobacteria have been observed in time-resolved experiments to rapidly respond to geochemical heterogeneity and experimental perturbations (i.e., colonization of fresh substrate) in hydrothermal vent systems (Alain et al. 2004; Sylvan et al. 2012a; b). Physiologies of specific groups of the Gammaproteobacteria often include oxidation of either sulfur or methane (Garrity et al. 2005;

Sorokin et al. 2007), both of which are common at settings with increased delivery of reduced fluids.

ANME-1 archaea, which are the most abundantly recovered ANME in the entire iTag dataset, exhibit wide ranges of relative abundance in both active and low-activity seep stations, with higher average relative abundance at low-activity stations, in agreement with previous clone library observations (Fig. 5; Marlow et al. 2014b). Similarly, the deltaproteobacterial family Desulfobacteraceae does not exhibit a clear difference in observed relative abundance as a function of seep activity (Fig. 5). It thus appears that some ANME-1 and deltaproteobacterial OTUs may be relatively insensitive to seepage level. This was unexpected as these are key taxa involved in the AOM process and therefore hypothesized to occur at higher relative abundance in methane-replete, presumably "active", seep stations. ANME-1 may be performing methanotrophy even within carbonates at low-activity stations, consistent with recent reports of AOM associated with carbonates on the periphery of active seepage (Marlow et al. 2014a). Alternatively, relic DNA from AOM-associated organisms may be preserved within carbonate rocks, as the carbonate precipitation process causes self-entombment, potentially sealing off inhabited pores (Stadnitskaia et al. 2005; Heijs et al. 2006; Marlow et al. 2014b; 2015). Evidence for biomarker preservation within carbonates has been described for lipids, which are more recalcitrant to degradation than DNA (Thiel et al. 2001; Stadnitskaia et al. 2005; Blumenberg et al. 2015).

2.4.3 DEMONSTRATION OF SUCCESSIONAL DYNAMICS: TRANSPLANTATION EXPERIMENTS

The "snapshot" view of carbonate-associated microbial ecology is augmented by the seafloor transplantation experiments, which allow us to observe *in situ* microbial successional patterns by simulating seep quiescence and activation. *In situ* flux measurements at Hydrate Ridge

have shown that seep activity can shift on week- to month-long timescales (Tryon et al. 1999; 2002), indicating our 13-month transplantation experiments are relevant to contemporary processes at Hydrate Ridge and potentially in other methane seep regions.

The OTU composition of the four active-to-low-activity transplanted microbial assemblages are statistically differentiable from both the native, active carbonate-associated microbial assemblages ($R=0.32$, $p=0.008$) as well as the native, low-activity carbonate-associated assemblages ($R=0.88$, $p<0.001$; Table S2; Fig. 1B). The four microbial assemblages transplanted from active to low-activity stations are more similar to the native, active carbonate assemblages (i.e., from where they originated) than to the native low-activity assemblages (i.e., to where they were transplanted, Fig 2B and ANOSIM results). The four transplanted carbonates exhibit approximately 30% lower overall OTU richness as compared to native carbonates (Fig. 2B), but in-depth analysis of OTU overlap between transplanted and native carbonates reveals a level of fine structure to the microbial turnover and succession (Fig. 4B-C). At the paired HR-3/-4 and HR-7/-8 stations, 68% and 52%, respectively, of the OTUs associated with native, active control carbonates are not recovered upon simulated seep quiescence after 13 months (Table S3). The "lost" OTUs are supplanted by characteristic OTUs gained from the low-activity sites (28 and 37 OTUs, representing 18% and 17% of the recovered OTUs for HR-3/-4 and HR-7/-8 transplants, respectively) as well as OTUs unique to the transplants and not recovered from native carbonates (20 and 24 OTUs for HR-3/-4 and HR-7/-8, respectively; Table S3). Nearly half of the OTUs recovered among the HR-3/-4 and HR-7/-8 transplants were cosmopolitan OTUs that were also observed in both the native, active and native, low-activity carbonates (Fig. 4B-C; Table S3). Thus, a loss of over half the initial OTUs upon seep quiescence is masked by gain of new OTUs, both unique and shared with the low-activity controls.

Combining the observation of overall similarity to native, active assemblages, diminished overall OTU richness, and specific turnover among the carbonates transplanted to low-activity stations, we can begin to paint a picture of microbial succession upon seep quiescence. Most

major (i.e., highly abundant) constituent members of carbonate-associated microbial assemblages are resilient to one year of quiescence (or their DNA doesn't degrade), as evidenced by the fact that transplanted carbonates plot among the native, active controls in Fig. 1B. Indeed, of the four carbonates transplanted to low-activity sites, we observe that 49-90% of the recovered sequences are from resilient OTUs shared with the active-station controls (Table S3). However, over the course of a year, low-abundance assemblage members are vulnerable to cessation of seep activity: the average relative abundance of lost OTUs in the native, active controls upon simulated quiescence was <0.5% (Table S3).

Examining specific taxa of interest, we find the gammaproteobacterial Thiotrichaceae OTUs remain at a similar relative abundance as the native, active carbonates, consistent with resilience to seep quiescence (Fig. 5). In contrast, epsilonproteobacterial Helicobacteriaceae OTUs that are highly abundant in native, active carbonates had mostly disappeared after 13 months of simulated seep quiescence (Fig. 5). Thus, two putative sulfur-oxidizing groups exhibit different 16S rRNA gene distribution, highlighting the potential for variable response to environmental change, even among taxa putatively belonging to the same guild. ANME-1 OTUs were recovered at high relative abundance in the carbonates transplanted to low-activity stations, consistent with the trend observed in native, low-activity carbonates and suggesting an ability to respond over a period of time that may represent, to ANME archaea, only a few generations (Girguis et al. 2003; Orphan et al. 2009; Morono et al. 2011).

The two carbonates which experienced simulated seep activation (transplanted from low-activity to active stations) host microbial assemblages different from low-activity, native carbonates and somewhat similar to native, active assemblages (Fig. 1B), although this experimental set suffers from low sample number associated with technical difficulties in recovering two of four originally transplanted carbonates. In juxtaposition to seep quiescence, which demonstrated resilience of the bulk microbial assemblages, our simulation of seep activation indicates that assemblages are relatively quick to respond to renewed seepage

conditions. This is especially true among the epsilonproteobacterial Helicobacteraceae OTUs, which are recovered in high relative abundance in the transplant-to-active carbonates, despite low relative abundance in the low-activity carbonates (Fig. 5). Other OTUs, for example gammaproteobacterial Thiotrichaceae, clearly demonstrate a slower response to seep activation (Fig. 5). Examination of two OTUs of putatively heterotrophic Chloroflexi, the Anaerolineaceae and Caldilineaceae, also reveals slow response to seep activation, despite their relatively high recovery among native, active seep carbonates (Fig. 5). The Anaerolineaceae OTU also exhibits markedly higher tolerance to low-activity conditions than the Caldilineaceae OTU (Fig. 5), highlighting the potential for different ecological expression among groups of similar phylogeny.

The coupled transplant experiments provide strong evidence that many carbonate-associated seep microbial taxa are adapted to cycles of seep quiescence and activation. This may be ecologically advantageous in an environment where fluid flow has a tendency to fluctuate rapidly and frequently (Tryon et al. 1999; 2002). Recalcitrance to seep quiescence is consistent with low but measurable AOM from carbonates at low-activity stations (Marlow et al. 2014a), and the physical buffering provided by carbonate habitats has been proposed as a factor for maintenance of microbial assemblage viability during periods of diminished seepage (Marlow et al. 2015). Alternatively, we note that 3 of the 4 carbonates transplanted from active to low-activity stations were composed of a mix of calcite and dolomite – mineralogies more common at active stations than low-activity stations (Fig. S4). If mineralogy significantly drives microbial composition, the observed recalcitrance to community shift may be explained by the fact that the transplanted carbonates bore mineralogies qualitatively associated with "active-seep-type" microbial assemblages. In contrast, the two samples transplanted from low-activity to active stations were aragonite/calcite mixes – a mineralogical composition regularly recovered from all seep stations regardless of activity (Fig. S4). Thus, the observed shift to an "active-seep-type" community is more likely a function of the seep activity shift than of mineralogy. The rapid microbial rebound upon simulated seep activation may be analogous to previous observations of

microbial community activation from deep terrestrial and marine subsurface environments (Morono et al. 2011; Rajala et al. 2015). Species richness in carbonates transplanted to active stations is higher than the reciprocal transplants – though still lower than native carbonates – further indicating microbial assemblage responsiveness to simulated seep activation (Fig. 2B). Diminished OTU richness upon transplantation (in either direction) is also evidence against a "time-integrative" model of carbonate microbial assemblages: if carbonates were passive recorders of all historic seep microbial DNA, OTU richness would not be expected to decrease.

2.4.4 DEMONSTRATION OF SUCCESSIONAL DYNAMICS: COLONIZATION EXPERIMENTS

Though our transplantation experiments best simulate the temporal variability of seepage for established microbial assemblages, they are limited in scope. To increase the interpretative power of our dataset, we supplemented the transplant experiments with carbonate (calcite and dolomite) and wood (fir and pine) colonization experiments to address the successional patterns and responsiveness of seep microorganisms colonizing at the seabed under conditions of differing seep activity and colonization substrate type.

Results from these experiments follow similar trends observed in the survey of native microbial assemblages where both habitat substrate ($R_{\text{carbonate vs wood}}=0.63$, $p<0.001$) and seep activity ($R_{\text{active vs low-activity}}=0.38$, $p<0.001$) differentiate the recovered microbial diversity (Fig. 1C, Table S2). In contrast to the survey of native carbonates, mineralogy did not contribute significantly to differences in total colonizing assemblage diversity ($p=0.109$; Table S2), further suggesting that the relationship between mineralogy and microbial diversity in the native carbonates may be due to a qualitative link between mineralogy and seep activity (Fig. S4). Microbial assemblages colonizing carbonates exhibited higher OTU richness and evenness than

those colonizing wood (Fig. 2C, Fig. S2C-D), substantiating the role of seep carbonates, specifically, as hosts of diverse microbial populations.

While hosting comparable OTU richness to the native carbonates (Fig. 2), the microbial assemblages colonizing the sterile carbonates at the seabed were, after 13 months, significantly different from native microbial assemblages collected in this study ($R=0.65$, $p<0.001$, Table S2; Fig. 1B). This supports general trends in the transplant experiments, suggesting that more than 13 months are required to achieve a mature successional phase if it is assumed that given enough time the colonizing assemblages would eventually mimic the native assemblages. Alternatively the colonization carbonates might never host microbial assemblages completely similar to the native carbonates, considering the different history of colonization (located at the seabed) and native (believed to have formed within the sediment column and later to have been exhumed) carbonates. Notably, however, sterile carbonates incubated at the seafloor share most of their observed OTUs with the native carbonates (Fig. 4D-I). The discrepancy between colonization and native carbonates hosting quite different microbial assemblages (Fig. 1B) and yet sharing many OTUs (Fig. 4D-I) implies assemblage differences are generally a function of differential OTU relative abundance, not of presence/absence of different OTUs themselves. Indeed, an ANOSIM test on presence/absence-normalized data reveals a diminished, though still significant, strength of difference between native and colonized carbonate microbial assemblages ($R=0.53$, $p<0.001$). In further support, among the six colonization/native pairings examined in detail (Fig. 4D-I), the majority (average 63%, range 46-84%, $n_{\text{colonization samples}}=12$) of the recovered colonization sequences were from OTUs shared between the colonization and native carbonates.

In-depth analysis of OTU overlap at station HR-9, chosen because of the wide array of habitat types and experimental samples obtained there, reveals that of the various OTUs shared between native and colonized carbonate assemblages, many are also shared with sediment and nodule assemblages (Fig. S6). This suggests some transference of sediment-hosted microbes onto the colonization carbonates. The mode of transfer is currently not known but may be associated

with direct microbial motility (Bernard and Fenchel 1995; Sievert et al. 2007), macrofaunal grazing/bioturbation (Bernard and Fenchel 1995; Thurber et al. 2012), and/or advection from fluid flow or gas ebullition (Schmale et al. 2015). At station HR-9, where 376 OTUs were reproducibly recovered from both colonization carbonates, 19% (n=71), 3% (n=11), and 4% (n=14) were exclusively sourced from carbonates, sediments/nodules, and bottom waters, respectively. The bottom-water samples, associated with this station, contained 1%-2% relative abundance of an OTU associated with the gammaproteobacterial Colwelliaceae, which were also recovered at moderate relative abundances from the colonization carbonates (<1% up to 20%; Table S3; Fig. 5) despite a lack of detection on either native or transplanted carbonates. This further indicates some transference of bottom water microorganisms onto carbonates during early-phase succession, and is consistent with common ecophysiology of Colwellia as generally marine, psychrophilic, motile, chemoorganotrophic microorganisms (Garrity et al. 2005). Thus, OTU recovery from multiple nearby substrates, coupled to the observed difference between colonized carbonate and wood microbial assemblages after 13 months ($R=0.63$, $p<0.001$; Fig. 1C) could be explained by two hypotheses: either (1) OTUs are recruited from all surrounding habitats, followed by assemblage differentiation according to habitat substrate (i.e., carbonates diverge from woods), or (2) carbonate colonization is a substrate-specific process from the very first microbial succession, and then over time occasional passive capture of OTUs from other habitat substrates occurs. In either case, the colonization data support the observation from native samples that carbonates host distinct microbial assemblages. Furthermore, carbonate distinctiveness is not simply a product of time-integrated passive capture of sediment-hosted microorganisms, nor does it depend on a history of burial in sediment.

Microbial diversity within the carbonate colonization experiments is almost wholly explained by seep activity differences, in further support of observations from native carbonates (Fig. 1C, $R=0.81$, $p<0.001$). Indeed, OTUs associated with the epsilonproteobacterial Helicobacteraceae exhibit a wide range of relative abundances in the colonization carbonates at

active stations, but only a very minor amount of colonization at low-activity stations (Fig. 5; Table S3). The Thiotrichaceae OTUs also demonstrate colonization patterns reminiscent of distributions observed in the native carbonates, again indicating that putative sulfur-oxidizing OTUs are dynamic responders to carbonate substrate availability in regions of seep activity at the seabed. However, the specific Thiotrichaceae OTU observed to most strongly colonize experimental carbonates was different than the Thiotrichaceae OTU more frequently observed in the native carbonates (Table S3) – demonstrating the potential for within-group variability in ecological expression. The recovery of Helicobacteraceae or Thiotrichaceae OTUs was not obviously tied to qualitative observations of bacterial mats upon recovery of colonized carbonates from the seafloor. Previous studies of microbial colonization in shallow marine sediments and near hydrothermal vents have observed a dominance of early-stage colonization by Epsilonproteobacteria (Bernard and Fenchel 1995; Taylor et al. 1999; Alain et al. 2004; Sylvan et al. 2012a), and similar ecological behavior appears to be occurring in methane seeps. The rapid colonization by Epsilonproteobacteria in various marine settings has been attributed to both a tolerance for rapidly changing physico-chemical conditions and motility within many members of the class (Bernard and Fenchel 1995; Alain et al. 2004). We observe that our key Helicobacteraceae OTUs were recovered in high relative abundance in methane seep sediments and low relative abundance in bottom water samples (Table S3); therefore, it appears likely that the Helicobacteraceae recovered in the colonization experiments were inoculated from underlying sediments, in contrast to Colwelliaceae OTUs derived from overlying bottom waters.

Colonization by the ANME-1-associated OTUs (the same OTUs as recovered from native carbonates) on the sterile carbonates was observed at low levels at both active and low-activity stations (Fig. 5). Any level of colonization by ANME-1 is intriguing for two reasons. First, ANME-1 are believed to have doubling times on the order of several months, so the 13-month course of the colonization experiments could reasonably be expected not to have provided enough time for ANME-1 archaea to colonize and become established on the fresh carbonate

substrates (Girguis et al. 2003; Orphan et al. 2009; Morono et al. 2011). Second, ANME-1 are obligate anaerobes typically associated with highly reducing conditions located deeper within the sediment column at seeps and near the sulfate-methane transition zone, not at the sediment/water interface where the colonization experiments were located (Knittel et al. 2005). An exception to this are the Black Sea 'reefs', composed partly of ANME-1; however, these grow into permanently stratified bottom water of the euxinic Black Sea (Reitner et al. 2005). That ANME-1 OTUs are observed at significant levels in the sediment samples but at negligible levels in the aerobic bottom water samples (Fig. 3) indicates that ANME-1 are almost certainly colonizing the carbonates seeded by the underlying sediments. This highlights the complexity of potential mechanisms driving regional and global between-seep dispersion of ANME-1 archaea and perhaps other ANME sub-clades, as previously observed (Ruff et al. 2015) and perhaps accomplished through periodic sediment disturbance. In contrast to our observations, Archaea were not observed as early colonizers in hydrothermal vent colonization experiments, despite their presence within *in situ* vent communities (Alain et al. 2004). Our experiments suggest that ANME-1 archaea may exhibit phenotypes thus far undiscovered in seep settings, or may be distributed by hydrological flow or macrofaunal movements (pumping, filtering, burrowing, defecation, etc.).

Wood-colonizing microbial assemblages at methane seeps in the Mediterranean Sea have been observed to be different than surrounding, off-seep sediment-hosted microbial assemblages (Bienhold et al. 2013). Our data further demonstrate that even among active and low-activity seep stations, wood-colonizing microbial assemblages differ after 13 months (Fig. 1C). The stark difference between carbonate- and wood-colonizing assemblages in our dataset highlights the importance of habitat substrate to deep-sea microbial assemblages. The mere presence of putative sulfur-oxidizing Epsilon-, and Gammaproteobacteria in the wood colonization experiments suggests wood-falls may act as ephemeral sulfide-rich reducing habitats, possibly representing stepping stones between seeps and vents for chemosynthetic communities as has been

hypothesized for metazoans and Bacteria (Distel et al. 2000; Bienhold et al. 2013). Our results are consistent with previous characterizations of native wood-fall samples, as well as deep-sea benthic wood colonization experiments, which yielded observations of phylogenetically diverse microbial assemblages including, but not limited to, the Bacteroidetes, Firmicutes, Spirochaetes, Epsilon-, and Gammaproteobacteria (Fagervold et al. 2012; Bienhold et al. 2013; Fagervold et al. 2014), but very limited recovery of methanogenic and methanotrophic archaeal taxa (Fagervold et al. 2012). The lack of significant ANME colonization in the wood experiments (Table S3) indicates that AOM-related archaeal taxa may have more difficulty spreading geographically via wood substrates than many Bacteria. That AOM-related archaeal taxa appear to be able to colonize carbonate substrates, even on relatively short timescales, indicates a possible mode of wide geographic dispersion. Other hypotheses have included transportation in the guts of deep-sea metazoans or distribution during ocean anoxic events (Ruff et al. 2015), both of which may complement the apparent suitability of carbonate habitats for ANME.

2.5 CONCLUSIONS

In summary the deployment of *in situ* manipulation experiments, coupled to an extensive characterization of native microbial assemblages in association with varying seep habitat substrates, has enabled unique insights into the ecology of seep microorganisms. Microbial assemblages associated with carbonates at methane seeps are distinct from, and more diverse than, other habitat substrates examined in this study, i.e., sediments, nodules, and bottom waters. Further, bulk carbonate-associated microbial assemblages are adapted to resist seep quiescence and poised to respond to seep activation over 13 months. OTUs associated with the epsilonproteobacterial Helicobacteraceae are particularly sensitive to seep activity. Colonization experiments corroborate that carbonates host distinct and diverse microbial assemblages, and

recovery of ANME-1 OTUs associated with the carbonates suggests more dynamic physiologies and/or distribution processes for these organisms than previously hypothesized.

The difference in the microbial assemblages associated with native active and low-activity carbonates, coupled to the dynamics and decreased OTU richness observed in the transplant experiments, suggests that upon the final quiescence of a historic methane seep, the genomic microbial signatures recorded in carbonates could differ from those microbes which were present during active seepage. Investigation of our same research questions should be applied to lipid profiles, to investigate whether trends observed at the genomic level are likely to be preserved in the rock record; in particular, whether microbial signatures in the rock record merely reflect the final, low-activity period of seep activity rather than the biological assemblage present during the most active phases of seepage and AOM.

2.6 ACKNOWLEDGMENTS

We thank Connor Skennerton and Elizabeth Trembath-Reichert for helpful discussion on data processing. We acknowledge Stephanie Connon, Patricia Tavormina, Josh Steele, Heather Grotzinger, and shipboard teams from the Orphan, Levin, Rathburn, and Rouse labs for assistance with sample collection and processing. We are indebted to the captain, crew, and pilots of the DSV Alvin and ROV Jason II from cruises AT15-11, AT15-44, AT15-68 who made this work possible. We thank the two anonymous reviewers whose comments strengthened the study. This research was supported by a grant to VO from the NASA Astrobiology Institute (Award # NNA13AA92A). This is NAI-Life Underground Publication Number 053. This work was also support by a National Science Foundation (NSF) grant (OCE-0825791) and a Gordon and Betty Moore Foundation, Marine Microbiology Initiative grant (#3780) to VO. DC was supported by a NSF Graduate Research Fellowship. Levin lab research was supported by NSF grants OCE-0826254 and OCE-0939557.

2.7 FIGURES

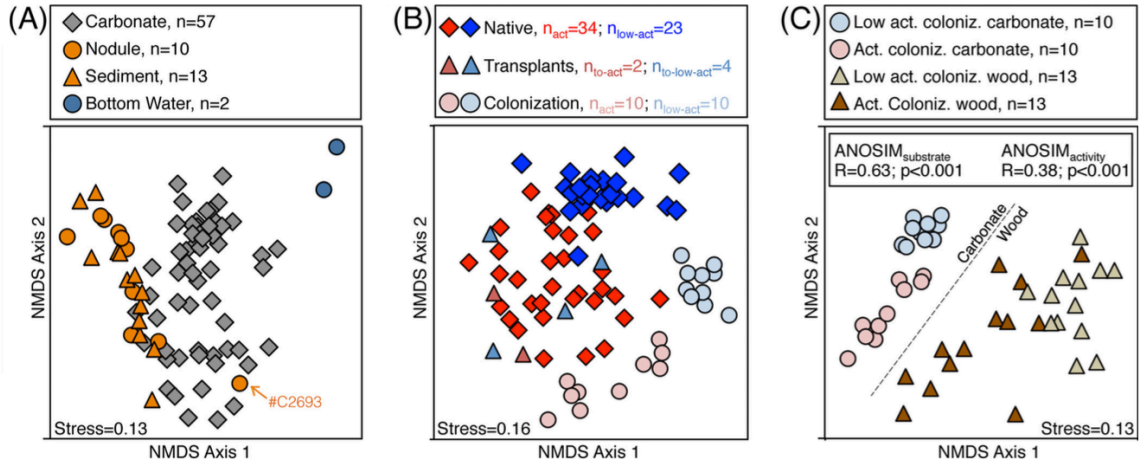

Fig. 1. Non-metric multidimensional scaling ordination of microbial assemblages in this study. Each point represents the entire recovered microbiological assemblage from one sample; samples plotting closer to each other are more similar in microbial composition. Lower stress values indicate better representation of the inter-sample (dis)similarities in two dimensions. (A) Native, unperturbed samples of sediment, nodule, bottom water, and carbonate habitat substrates. Sample #C2693 (identified by orange arrow) represents a nodule-hosted microbial assemblage recently determined to be a biological outlier among sediment and nodules (Mason et al., 2015). (B) Ordination of only carbonate samples, representing the native, transplantation, and colonization treatments. (C) Ordination of only colonization samples, representing carbonate and wood substrates at active and low-activity stations. We cannot rule out that in subplot (A), bottom water microbial assemblages could be different than sediments, nodules, and carbonates because they were extracted by a different method; the same could be true for the observed difference between carbonate- and wood-hosted assemblages in subplot (C).

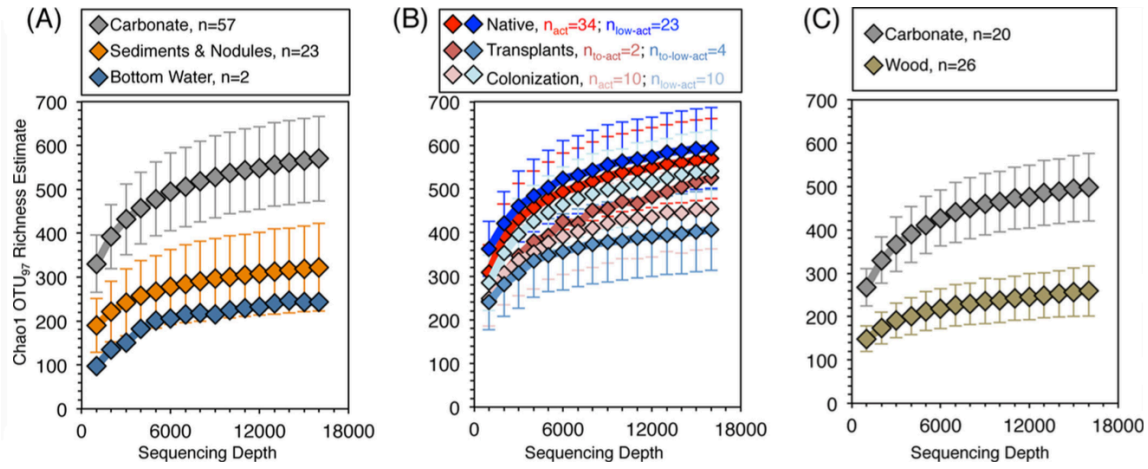

Fig. 2. Collector's curves of estimated Chao1 OTU_{97} richness. 1σ standard deviations are given by the y-axis error bars. (A) Native microbial assemblages associated with carbonates, sediments and nodules, and the two bottom water samples. Sediments and nodules were binned as one group because their associated microbial assemblages were indistinguishable according to ANOSIM tests (Table S2). (B) Carbonate samples in this study, separated by treatment category. (C) Carbonate and wood colonization samples. Standard deviations are not given for bottom water and transplant-to-active sample groups, due to the low number of analyzed samples. Raw OTU rarefaction curves are given in Fig. S2A-C.

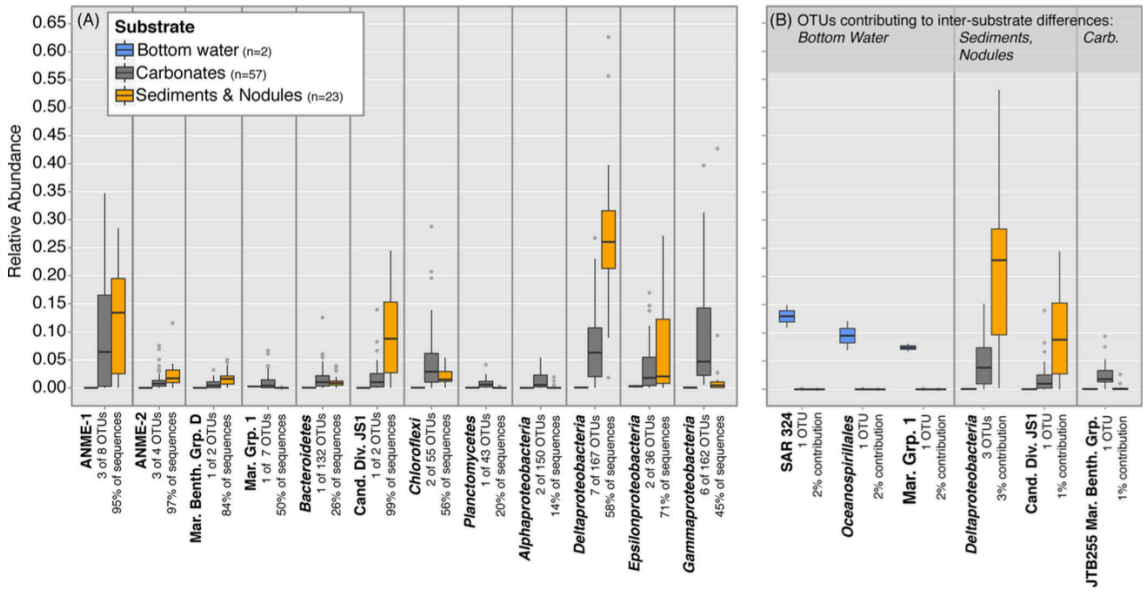

Fig. 3. Boxplot of OTU relative abundances from the 82 native samples in this study. Sediments and nodules are binned as one group because ANOSIM tests revealed their associated microbial assemblages to be statistically indistinguishable. Boxplot centerline represents the median (50th percentile, Q_{50}). The top and bottom hinges represent Q_{75} and Q_{25} quartiles, respectively. The upper and lower whiskers correspond to the highest and lowest data points within 1.5 times the Inter-Quartile Range (Q_{75} minus Q_{25}) from the median. Any data points outside of that range are identified by gray dots. The same plotting format is applied to Fig. 5. (A) Relative abundances of the top 30 most abundant OTUs in the dataset, grouped by taxonomy. The full dataset contains 1,057 OTUs, but the top 30 OTUs account for 1%, 67%, and 43% of the sequences recovered from bottom water, sediment/nodule, and carbonate substrates, respectively. (B) Relative abundances of OTUs revealed to be strongly associated with particular habitat substrates. Inter-substrate differences in microbial assemblages are a cumulative result of contributions from many OTUs; even OTUs strongly associated with a particular habitat substrate only contribute several percent to the total inter-substrate variability. Note that the JS1 OTU is the same in panels (A) and (B) – it is both highly abundant and strongly associated with sediments and nodules. The Marine Group 1 OTU in panels (A) and (B) is different – there is one Marine Group 1 OTU highly abundant in the dataset, subpanel (A), and another Marine Group 1 OTU strongly associated with bottom water samples, subpanel (B). This highlights the variable distribution of phylogenetically similar OTUs. The y-axis of panel (A) also applies to panel (B). Raw OTU data used to generate this plot is available in Table S3.

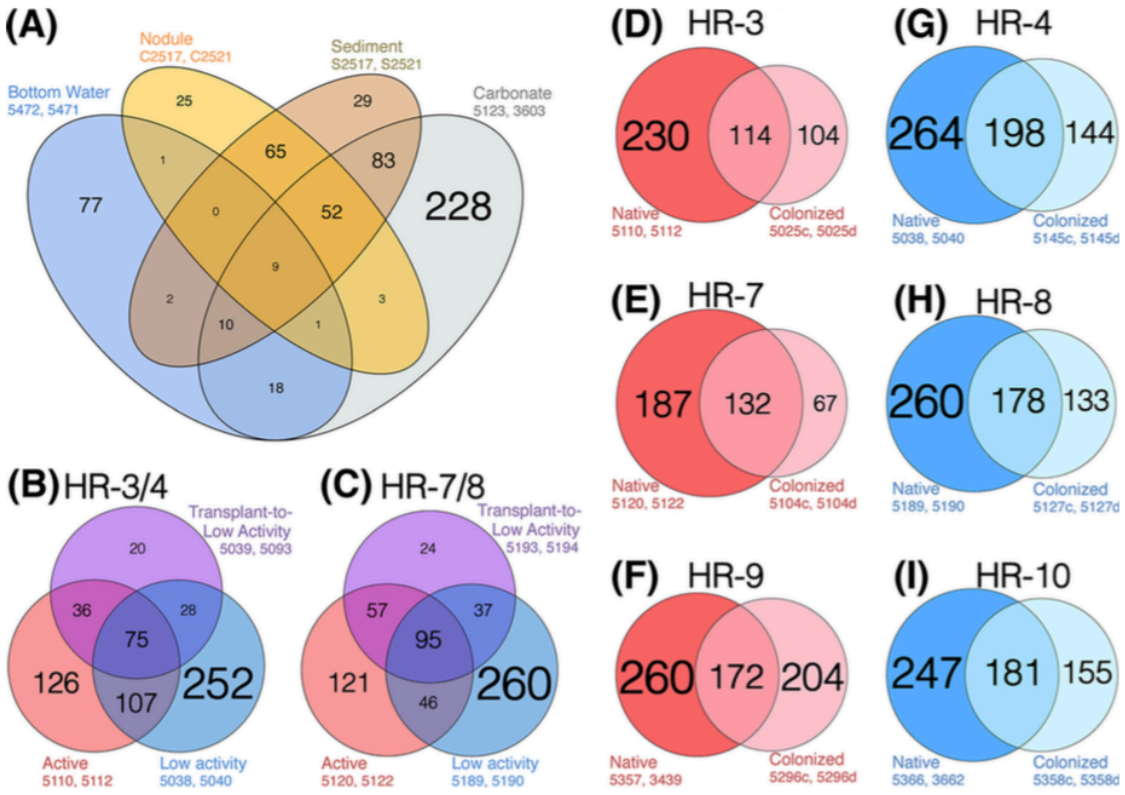

Fig. 4. Comparison of OTU_{97} overlap among various samples and treatments. In order to ensure equal depth of sampling across each substrate type, two representative samples of each substrate were chosen randomly (see sample numbers on the Figure). **(A)** OTU overlap between the four native seep habitat substrates examined in this study: sediments, nodules, carbonates, and bottom water. In order to minimize geographic bias in the analysis, samples were chosen from active stations at Hydrate Ridge South (the only exception was Bottom Water sample #5472, which was from an HR-South low-activity station). Note that carbonates host the richest OTU diversity (c.f. the collector's curve in Fig. 2A), including a large number of OTUs which are distinct to carbonates. Carbonates share more OTUs with sediments and nodules than with bottom waters, possibly indicative of an origin within the sediment column and subsequent exhumation and exposure at the seafloor. Bottom waters contribute more OTUs to carbonates than to either sediments or nodules – consistent with the recovery of our carbonates from directly on the seafloor. (B-C) OTU overlap of active and low-activity control carbonates, and transplant-to-low-activity carbonates, for the HR-3/-4 and HR-7/-8 transplant experiments. Transplant-to-active carbonates were not included due to their low sample number (n=1 for each of HR-3/-4 and HR-7/-8). (D-I) OTUs observed in native carbonate samples vs colonized carbonate samples as a function of Hydrate Ridge station. Stations were included only if they received colonization carbonate deployments *and* we had recovered native carbonates from the same station (these criteria excluded HR-1, HR-2, HR-6, HR-11, and the Southeast Knoll). Left column (red, D-F) are active stations, right column (blue, G-I) are low-activity stations. In each case, the bold color represents the native carbonates and the pale color represents the colonized carbonates. The number in each region denotes the number of OTUs, and font and circle sizes are proportional to OTU count. In most cases, the majority of recovered OTUs from colonization carbonates were also present in native carbonates.

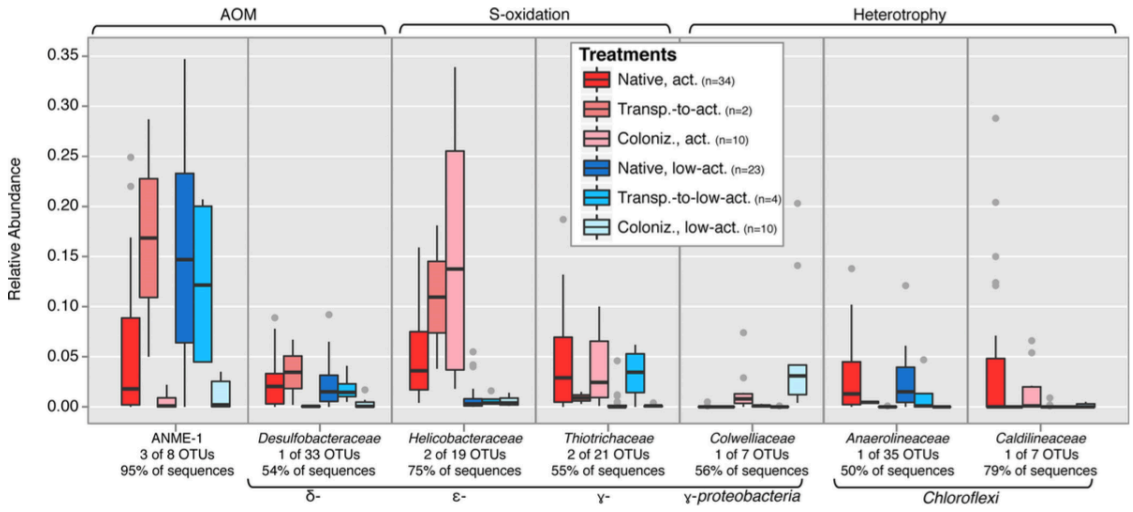

Fig. 5. Boxplot of carbonate-associated relative abundance data of selected key OTUs identified by SIMPER, representing notable taxonomic groups. Note that data for some groups are combined from several OTUs (OTU data are reported individually in Table S3). Although in all cases a minority of the OTUs were identified for presentation (e.g., 3 of 8 for ANME-1), these generally represented the majority of the total sequences recovered among each taxonomy (e.g., 95% of all sequences for ANME-1). When generated with all OTUs associated with each taxa, this plot does not change substantially (data not shown).

2.8 SUPPLEMENTAL MATERIAL: TEXT

2.8.1 SEEP STATION CHARACTERIZATION: ACTIVE vs LOW-ACTIVITY STATION DESIGNATIONS

Higher seep activity is associated with a higher delivery of reduced fluids, including methane and sulfide, from the subsurface. Although common geochemical measurements such as sulfide concentration are difficult to recover from directly below seep carbonates, pore water sulfide concentrations from nearby 0-3 centimeter-below-seafloor (cmbsf) horizons of sediment cores reveal a wide range of concentrations at our active stations (1-14 mM range, 6 mM average, n=9, data from HR-3, -7, -9, and -V1), whereas 0-3 cmbsf horizons of low activity stations contained <1 mM sulfide (0.2 mM average, n=5, data from HR-4 and -V2) (raw data unpublished). Station HR-V2 did not contain any samples used for analysis in this study, so will not be found in Table S1, but represented a seafloor low-activity station not unlike other low-activity stations in this study. Station HR-V2 was located at 44.570374°N, 125.14683°W (HR-South).

Those measured sulfide concentrations are consistent with previous studies of methane seeps (Gieskes et al. 2005; Green-Saxena et al. 2014; Pop Ristova et al. 2015), corroborate our active vs low activity designations, and also support published measurements of AOM in low-activity seep carbonates and sediments (Marlow et al. 2014a). Carbonates have been shown to adsorb methane, resulting in concentrations of methane 100-fold higher than the surrounding sediment (Ijiri et al. 2009). Therefore in areas of active seepage, carbonates might be a particularly methane-replete habitat substrate, magnifying the contrast with methane-depleted conditions in sediments from low-activity seepage areas.

2.8.2 X-RAY DIFFRACTION (XRD)

Among the 57 native seep carbonate samples in this study, 56 were mineralogically characterized (1 lacked enough material for XRD analysis). All six and all twenty of the transplant and colonization carbonates, respectively, were also characterized by XRD. Carbonate powders were analyzed on a Phillips X'Pert Multi Purpose X-Ray Diffractometer in the Division of Applied Physics and Materials Science at Caltech. Measurements were taken from 10˚ to 70˚ 2θ with step size of 0.05˚. SiO_2 standards were run to confirm peak location accuracy. For correlation with microbial assemblage data, samples were coarsely binned into groups based on the presence/absence of diagnostic (104), (221), and (104) peaks for calcite, aragonite, and dolomite respectively (Kontoyannis and Vagenas 2000; Zhang et al. 2010; Marlow et al. 2014b). The results of this mineralogical binning are reported in Table S1, and visualized in Fig. S5 for the native carbonates.

We note a qualitative, apparent correlation between mineralogy and seep station activity (Fig. S4). Low-activity stations are dominated by aragonite-bearing carbonate mineralogies, while active seep stations demonstrate higher carbonate mineralogical variability, including a large proportion of samples found to contain dolomite. Related to this qualitative correlation, we find a strong statistical differentiation of the native carbonate-associated microbial assemblages according to both seep activity and mineralogy (Table S2, see R values). While being sure to note that both seep activity and mineralogy differentiate the native carbonate dataset in the main text of the manuscript, we chose to focus the discussion around the indicator variable of seep activity because it was according to this environmental variable that we explicitly deployed the transplant and colonization experiments.

The links between microbial assemblage, seep activity, and mineralogy remain unresolved and an active area of research. Addressing and illuminating such links is not in the scope of this particular study, although it continues to be a focus of inquiry in our research

program. Broadly, seep activity and mineralogy are hypothesized to be linked to sulfate inhibition of Mg-bearing carbonate phases during precipitation (Peckmann et al. 2001; Naehr et al. 2007; Krause et al. 2012; Bian et al. 2013). However, a variety of outstanding questions remain: Do new carbonates precipitate at low-activity sites even after "high" levels of seepage disappear? What role does secondary alteration play in seep carbonates, and on what timescale? Is carbonate mineralogy further linked to depth and/or microbial regime in the sediment column, and how can this be interpreted or inferred by collecting samples directly from the seafloor? Do particular microorganisms prefer particular carbonate mineralogies, or is the biological differentiation we observe in our dataset mechanistically linked to other environmental parameters (i.e., seep activity)? If microorganisms demonstrate carbonate mineralogical preferences, is this due to chemical or physical aspects of mineralogy?

2.8.3 TRANSPLANTATION AND COLONIZATION DESCRIPTIONS

Exposed carbonates were selected on the seafloor during DSV Alvin dives AD4630, '31, '32 and '34 at HR-North in August 2010 for transplantation. Selected carbonates were picked up with the submersible's arm, temporarily deposited in the payload chassis, and deployed at selected destinations with a marked, weighted stake. The time-intensive nature of this effort, coupled with the difficulty of irrefutably re-identifying transplanted carbonates for recovery 13 months later, limited the total sample number of transplantation experiments. Ultimately, four carbonates were transplanted from active to low activity sites and subsequently recovered, and two from low activity to active sites (two other carbonates which were transplanted from low activity to active stations were unable to be successfully recovered). At each site, we established experimental control carbonates by using the DSV Alvin's manipulator arm to pick up native carbonates from the seafloor, and simply re-depositing them on the seafloor in their original location (identified in Table S1). Upon sequencing, these controls were indistinguishable from other native seep

carbonates (Table S2). Transplanted carbonates and controls were recovered in individual chassis compartments after 13 months during R/V Atlantis cruise 18-10 (September 2011), and frozen at -80˚C upon collection.

Since transplanted carbonates were moved from active- to low activity stations and vice versa, the effect of transplantation can be evaluated by comparing microbial assemblage similarity between the transplanted carbonates and the native, *in situ* carbonates binned into active and low-activity groups. This requires the assumption that the transplanted carbonates hosted an initial assemblage of microorganisms consistent with the characteristic assemblages associated with the native, active and native, low-activity carbonates in our study. This assumption is considered reasonable given the high sampling depth of native carbonates in this study and the strong difference between native microbial assemblages according to seep activity.

During a prior cruise in 2006, massive calcite and dolomite seep carbonates were recovered from Eel River Basin. After dry room temperature storage at Caltech for multiple years, the calcite and dolomite were each subsampled into 10 pieces of approximately 10^3 cm^3. These subsamples were autoclaved, stored aseptically, and brought to sea during R/V Atlantis cruise 15-68 in August 2010. XRD spectra of pre- and post-autoclaving mineral chips indicated no change in structure after sterilization. Pairs of one calcite and one dolomite subsample were deployed in a mesh bag on the seafloor at selected active and low-activity stations at Hydrate Ridge, adjacent to the transplant experimental rocks (Table S1). After 13 months of colonization, these carbonates were recovered in September 2011 during R/V Atlantis cruise 18-10. DNA extraction and PCR were unsuccessful on pre-colonization carbonate negative controls. If historic, remnant DNA were preserved in the colonization carbonates, and subsequently recovered during post-experimental DNA extraction and sequencing, then the colonization samples would not be expected to cluster according to seep activity and, most likely, would cluster within the suite of native carbonates in Fig. 1B and Fig. S3B. Neither of those null hypotheses are

true, further suggesting genuine deposition of new DNA material during the 13-month colonization experiments.

Twenty-six wood samples were also deployed for colonization during the same 13-month time interval. Natural pine (*Pinus* sp.) and natural douglas fir (*Pseudotsuga menziesi*) samples with bark were collected from forests in southwest Washington state, and non-treated wood blocks of douglas fir were purchased in San Diego, CA. Wood samples were deployed at sea in the same manner and at many of the same stations as the carbonate colonization experiments, but were not autoclaved prior to emplacement *in situ*. We are confident that our recovered 16S sequences from the wood experiments reflect genuine colonization (not microbes present prior to deployment) because the wood samples show biological differentiation according to seep activity (Fig. 1C), which would not be predicted from the microbial communities prior to being placed at active and low-activity stations. Furthermore, if any indigenous microbes were living in or on the wood, they were placed in a deep seafloor environment that would not be conducive to their terrestrial origins and growth. Finally, the recovered sequences from the wood samples are similar in composition to those observed in previous deep-sea wood colonization experiments (see Discussion in the main text)

2.8.4 PROCESSING OF MiSeq DATA

Raw sequence data for all 134 samples in this study can be accessed in the Sequence Read Archive under accession numbers SRP055767 and SRP049675. A sequential list of the in-house QIIME.1.8.0 commands used to process the data is given below.

1. Joining paired ends to generate contigs

```
join_paired_ends.py -f <sample_name_R1.fastq> -r
<sample_name_R2.fastq> -m fastq-join -j 50 -p 8 -o
<sample_name>_joined/
```

2. Quality trimming, converting from fastq to fasta format

```
split_libraries_fastq.py -i
<sample_name>_joined/fastqjoin.join.fastq -o
<sample_name>_trimmed/ -m dummy_mapping.txt --sample_id
<sample_name> -q 29 -n 0 --barcode_type 'not-barcoded' --
store_qual_scores
```

3. Chimera checking

```
usearch6.0.203_i86linux32 -uchime_ref
<sample_name>_trimmed/seqs.fna -db
SSURef_NR99_Silva_115_pintailF_ORPHAN.fasta -uchimeout
<sample_name>_chimerachecked/results.uchime --strand plus -
chimeras <sample_name>_chimerachecked/uchime_chimeras.fna -
nonchimeras <sample_name>_chimerachecked/uchime_nonchimeras.fna
```

4. Concatenating all sequences from all samples

```
cat *checked/uchime_nonchimeras.fna > all_seqs_all_samples.fasta
```

5. Picking OTUs at 97% similarity

```
pick_otus.py -i all_seqs_all_samples.fasta -s 0.97 -o
uclust_picked_otus_97/
```

6. Picking representative sequences for each OTU

```
pick_rep_set.py -i
uclust_picked_otus_97/all_seqs_all_samples_otus.txt -f
all_seqs_all_samples.fasta -m most_abundant
```

7. Assigning taxonomy for each OTU

```
assign_taxonomy.py -i all_seqs_all_samples.fasta_rep_set.fasta -t
SSURef_NR99_Silva_115_pintailF_ORPHAN.tax -r
SSURef_NR99_Silva_115_pintailF_ORPHAN.fasta --uclust_similarity
0.9 --uclust_max_accepts 10 --uclust_min_consensus_fraction 0.90
-o uclust_picked_otus_97/uclust_taxa_0.9_10_0.90/
```

8. Making OTU table in biom format

```
make_otu_table.py -i
uclust_picked_otus_97/all_seqs_all_samples_otus.txt -t
uclust_picked_otus_97/uclust_taxa_0.9_10_0.90/all_seqs_all_sample
s.fasta_rep_set_tax_assignments.txt -o
uclust_picked_otus_97/uclust_taxa_0.9_10_0.90/OTU_table_Silva_115
_all_seqs.biom
```

9. Removing singleton OTUs from the dataset

```
filter_otus_from_otu_table.py -i
uclust_picked_otus_97/uclust_taxa_0.9_10_0.90/OTU_table_Silva_115
_all_seqs.biom -n 2 -o
uclust_picked_otus_97/uclust_taxa_0.9_10_0.90/OTU_table_singleton
filtered.biom
```

10. Filtering known PCR contaminant taxa from the dataset by taxonomic name

```
filter_taxa_from_otu_table.py -i
uclust_picked_otus_97/uclust_taxa_0.9_10_0.90/OTU_table_singleton
filtered.biom -o
uclust_picked_otus_97/uclust_taxa_0.9_10_0.90/OTU_table_singleton
_taxafiltered.biom -n
Unassigned,Eukaryota,__Enterobacteriaceae,__Streptococcaceae,__Ps
eudomonadaceae,__Moraxellaceae,__Oxalobacteraceae
```

11. Generating Excel-readable OTU table with taxonomic information (*employs an in-house perl command written by Dr. Connor Skennerton)

```
join_otu_repset.pl
uclust_picked_otus_97/uclust_taxa_0.9_10_0.90/OTU_table_singleton
_taxafiltered.biom all_seqs_all_samples.fasta_rep_set.fasta >
OTU_table_wTaxa_wSeqs_97.txt
```

12. The Excel-readable table from Step 11 was used to identify the OTUs which represent poorly-defined Gammaproteobacteria (defined by QIIME as simply Bacteria;__Proteobacteria;__Gammaproteobacteria), and which have been shown to be PCR contaminants in internal lab control tests. This list of OTUs was then used in this step of filtering in QIIME. We could not simply remove "__Gammaproteobacteria" in Step 10 because it would have resulted in the loss of OTUs which represent genuine Gammaproteobacteria in our dataset. These poorly-defined Gammaproteobacteria represented an average of 4%±5% of the sequences per sample in our dataset.

```
filter_otus_from_otu_table.py -i
uclust_picked_otus_97/uclust_taxa_0.9_10_0.90/OTU_table_singleton
_taxafiltered.biom -e OTUs_to_exclude_GammaF_97.txt -o
uclust_picked_otus_97/uclust_taxa_0.9_10_0.90/OTU_table_singleton
_taxa_Gammafiltered.biom
```

13. Filtering OTUs which appear at less than 0.01% relative abundance in the entire dataset

```
filter_otus_from_otu_table.py -i
uclust_picked_otus_97/uclust_taxa_0.9_10_0.90/OTU_table_singleton
_taxa_Gammafiltered.biom --min_count_fraction 0.0001 -o
uclust_picked_otus_97/uclust_taxa_0.9_10_0.90/OTU_table_singleton
_taxa_Gamma_10000filtered.biom
```

14. Counting number of remaining sequences per sample to identify the level for rarefaction (found to be 16,051 sequences/sample, equal to the smallest sample)

```
biom summarize-table -i
uclust_picked_otus_97/uclust_taxa_0.9_10_0.90/OTU_table_singleton
_taxa_Gamma_10000filtered.biom -o
OTU_table_singleton_taxa_Gamma_10000filtered_SeqSummary.txt
```

15. Rarefying all samples down to the minimum number of sequences per sample

```
single_rarefaction.py -i
uclust_picked_otus_97/uclust_taxa_0.9_10_0.90/OTU_table_singleton
_taxa_Gamma_10000filtered.biom -d 16051 -o
uclust_picked_otus_97/uclust_taxa_0.9_10_0.90/OTU_table_singleton
_taxa_Gamma_10000_rarefied.biom
```

16. Generating Excel-readable OTU table for downstream alpha and beta diversity calculations

```
biom convert -i
uclust_picked_otus_97/uclust_taxa_0.9_10_0.90/OTU_table_singleton
_taxa_Gamma_10000_rarefied.biom -o
uclust_picked_otus_97/uclust_taxa_0.9_10_0.90/OTU_table_singleton
_taxa_Gamma_10000_rarefied.txt -b
```

2.8.5 NMDS, ANOSIM, & SIMPER TESTS IN R

Generic examples of the three commands are given below, including the options employed for this study. All commands require installation of the 'vegan' package in R, as well as two dependencies: 'lattice' and 'permute'. For this study, the following package versions were employed:

'vegan': v2.0-10
'lattice': v0.20-29
'permute': v0.8-3

1. NMDS

```
NMDS_analysis=metaMDS(sqrt_transformed_data,distance="bray",k=2,t
rymax=100,engine=c("monoMDS"),autotransform=FALSE)
```

2. ANOSIM

```
ANOSIM_analysis=with(sample_metadata,anosim(sqrt_transformed_data
,Activity,permutations=999,distance="bray"))
```

3. SIMPER

```
SIMPER_analysis=with(sample_metadata,simper(sqrt_transformed_data
,Activity))
```

2.9 SUPPLEMENTARY MATERIAL: TABLES

Supplementary Table 1-1. All samples in this study are listed with their accompanying metadata. Bold boxes denote the three different experimental treatments in the study: native samples, transplantation samples, and colonization samples.

Sample Number	Experimental Treatment	Habitat Substrate	Activity[c]	Regional Geography[a]	Specific Hydrate Ridge Geography	Local Geography	Latitude (Decimal °N)	Longitude (Decimal °W)	Depth (mbsl)	Habitat Substrate Sub-type[d]
5471		Bottom Water	Active	HR	South	HR-9	44.568466	125.152698	770	n.a.
5472			Low Activity	HR	South	off-HR-9	44.568511	125.151905	794	n.a.
3439		Carbonate	Active	HR	South	HR-9	44.568457	125.152761	775	A
3781				HR	South	HR-11	44.567899	125.153101	795	A
5357				HR	South	HR-9	44.568367	125.152774	774	A
5359				HR	South	HR-11	44.567782	125.153227	798	A
5436				HR	South	HR-11	44.567845	125.153038	794	A
2841				CR	n.a.	Mound 12	8.930590	84.312599	997	AC
2933				CR	n.a.	Mound 11	8.923242	84.303747	1010	AC
3138				CR	n.a.	Mound 12	8.930569	84.312839	996	AC
3530				HR	North	HR-3	44.669544	125.098057	587	AC
3626				HR	North	HR-7	44.667151	125.100020	602	AC
5330				HR	South	HR-V1	44.570239	125.147023	775	AC
5434				HR	South	HR-11	44.567890	125.153063	794	AC
5122[b]				HR	North	HR-7	44.667079	125.100033	601	AC
2781				CR	n.a.	Mound 12	8.929776	84.310799	989	ACD
3007				CR	n.a.	Quepos Mound	9.031787	84.621334	1402	C
3531				HR	North	HR-3	44.669544	125.098057	587	C
3532				HR	North	HR-3	44.669544	125.098057	587	C
3623				HR	North	HR-3	44.669499	125.098220	588	C
3544				HR	North	HR-7	44.667115	125.099995	602	CD
3602				HR	Southeast Knoll	n.a.	44.447635	125.028390	626	CD
3622				HR	North	HR-3	44.669499	125.098220	588	CD
3624				HR	North	HR-3	44.669499	125.098220	588	CD
3625				HR	North	HR-7	44.667151	125.100020	602	CD
3628				HR	North	HR-7	44.667151	125.100020	602	CD
5102				HR	North	HR-7	44.667106	125.099970	600	CD
5103				HR	North	HR-7	44.667106	125.099970	600	CD
5109[b]				HR	North	HR-3	44.669463	125.098120	587	CD
5110[b]				HR	North	HR-3	44.669481	125.098095	587	CD
5112[b]				HR	North	HR-3	44.669481	125.098107	587	CD
5123[b]				HR	North	HR-7	44.667079	125.100033	601	CD
3502				HR	North	HR-3	44.669535	125.098158	587	D
3603				HR	Southeast Knoll	n.a.	44.451163	125.027987	618	D
5120[b]				HR	North	HR-7	44.667079	125.100020	601	D
3665				HR	South	HR-9	44.568421	125.152786	775	n.m.
3079			Low Act.	CR	n.a.	Jaco Scarp	9.172603	84.798496	739	A
3599				HR	Southeast Knoll	n.a.	44.450632	125.029258	612	A
3662				HR	South	HR-10	44.568223	125.152987	778	A
5366				HR	South	HR-10	44.568178	125.152887	787	A
5038[b]				HR	North	HR-4	44.670075	125.098674	595	A
2874	Native			CR	n.a.	Mound 12	8.929939	84.310636	987	AC
2875				CR	n.a.	Mound 12	8.929939	84.312371	995	AC
2876				CR	n.a.	Mound 12	8.929866	84.313026	996	AC
3078				CR	n.a.	Jaco Scarp	9.172603	84.798496	739	AC
3464				HR	North	HR-4	44.670120	125.098686	592	AC
3511				HR	North	HR-5	44.669382	125.103619	620	AC
3541				HR	North	HR-8	44.667726	125.100838	603	AC
3543				HR	North	HR-8	44.667744	125.100926	602	AC
3627				HR	North	HR-8	44.667546	125.100763	603	AC
5153				HR	North	HR-8	44.667582	125.100712	602	AC
5040[b]				HR	North	HR-4	44.670075	125.098674	595	AC
5189[b]				HR	North	HR-8	44.667645	125.100712	604	AC
5190[b]				HR	North	HR-8	44.667645	125.100712	604	AC
3542				HR	North	HR-8	44.667726	125.100838	603	ACD
3545				HR	North	HR-8	44.667744	125.100926	602	ACD
3457				HR	North	HR-4	44.670057	125.098749	595	CD
3458				HR	North	HR-4	44.670057	125.098749	595	D
3604				HR	Southeast Knoll	n.a.	44.448670	125.030466	632	D
C2517[e]		Nodule	Active	HR	South	HR-V1	44.570059	125.147348	800	AC
C2518[e]				HR	South	HR-V1	44.570059	125.147348	800	AC
C2519[e]				HR	South	HR-V1	44.570059	125.147348	800	AC
C2521[e]				HR	South	HR-V1	44.570059	125.147348	800	C
C2689[e]				ERB	n.a.	n.a.	40.811495	124.610823	520	C
C2688[e]				ERB	n.a.	n.a.	40.811495	124.610823	520	CD
5118N				HR	North	HR-7	44.667061	125.099970	600	n.m.
C2520[e]				HR	South	HR-V1	44.570059	125.147348	800	n.m.
C2703[e]			Low Activity	ERB	n.a.	n.a.	40.811495	124.610823	520	CD
C2693[e]			Off-seep	ERB	n.a.	n.a.	40.811495	124.610823	520	C
2686		Sediment	Active	ERB	n.a.	n.a.	40.811495	124.610823	520	n.a.
2687				ERB	n.a.	n.a.	40.811495	124.610823	520	n.a.
5118				HR	North	HR-7	44.667061	125.099970	600	n.a.
S2517[e]				HR	South	HR-V1	44.570059	125.147348	800	n.a.
S2518[e]				HR	South	HR-V1	44.570059	125.147348	800	n.a.
S2519[e]				HR	South	HR-V1	44.570059	125.147348	800	n.a.
S2520[e]				HR	South	HR-V1	44.570059	125.147348	800	n.a.
S2521[e]				HR	South	HR-V1	44.570059	125.147348	800	n.a.
S2688[e]				ERB	n.a.	n.a.	40.811495	124.610823	520	n.a.
S2689[e]				ERB	n.a.	n.a.	40.811495	124.610823	520	n.a.
5163			Low Act.	HR	North	HR-8	44.667447	125.100486	601	n.a.
S2703[e]				ERB	n.a.	n.a.	40.811495	124.610823	520	n.a.
S2693[e]			Off-seep	ERB	n.a.	n.a.	40.811495	124.610823	520	n.a.

Supplementary Table 1-2. All samples in this study are listed with their accompanying metadata. Bold boxes denote the three different experimental treatments in the study: native samples, transplantation samples, and colonization samples.

Sample Number	Experimental Treatment	Habitat Substrate	Activity[c]	Regional Geography[a]	Specific Hydrate Ridge Geography	Local Geography	Latitude (Decimal °N)	Longitude (Decimal °W)	Depth (mbsl)	Habitat Substrate Sub-type[d]
5111	Transplantation	Carbonate	Low Act. -> Act.	HR	North	HR-3	44.669463	125.098120	587	AC
5121				HR	North	HR-7	44.667079	125.100020	601	AC
5193			Act. -> Low Act.	HR	North	HR-8	44.667627	125.100712	603	AC
5039				HR	North	HR-4	44.670093	125.098699	595	CD
5093				HR	North	HR-4	44.670084	125.098686	595	CD
5194				HR	North	HR-8	44.667627	125.100712	603	CD
5025c	Colonization	Carbonate	Active	HR	North	HR-3	44.669454	125.098145	588	C
5104c				HR	North	HR-7	44.667088	125.099995	600	C
5186c				HR	North	HR-6	44.668842	125.108653	613	C
5296c				HR	South	HR-9	44.568412	125.152786	774	C
5302c				HR	South	HR-1	44.568484	125.152635	774	C
5025d				HR	North	HR-3	44.669454	125.098145	588	D
5104d				HR	North	HR-7	44.667088	125.099995	600	D
5186d				HR	North	HR-6	44.668842	125.108653	613	D
5296d				HR	South	HR-9	44.568412	125.152786	774	D
5302d				HR	South	HR-1	44.568484	125.152635	774	D
5127c			Low Act.	HR	North	HR-8	44.667636	125.100737	602	C
5145c				HR	North	HR-4	44.670075	125.098661	600	C
5301c				HR	South	HR-2	44.570302	125.152786	810	C
5308c				HR	North	HR-5	44.669535	125.103946	618	C
5358c				HR	South	HR-10	44.568187	125.152899	788	C
5127d				HR	North	HR-8	44.667636	125.100737	602	D
5145d				HR	North	HR-4	44.670075	125.098661	600	D
5301d				HR	South	HR-2	44.570302	125.152786	810	D
5308d				HR	North	HR-5	44.669535	125.103946	618	D
5358d				HR	South	HR-10	44.568187	125.152899	788	D
5036		Wood	Active	HR	North	HR-3	44.669454	125.098145	588	DougFir
5106				HR	North	HR-7	44.667088	125.099995	600	DougFir
5187				HR	North	HR-6	44.668833	125.108653	613	DougFir
5295				HR	South	HR-9	44.568466	125.152824	775	DougFir
5298				HR	South	HR-1	44.568511	125.152648	774	DougFir
5368				HR	South	HR-11	44.567773	125.153277	800	DougFir
5030				HR	North	HR-3	44.669445	125.098132	588	NatFir
5108				HR	North	HR-7	44.667088	125.099995	600	NatFir
5188				HR	North	HR-6	44.668833	125.108678	613	NatFir
5293				HR	South	HR-9	44.568466	125.152824	775	NatFir
5037				HR	North	HR-3	44.669445	125.098145	588	NatPine
5107				HR	North	HR-7	44.667088	125.099995	600	NatPine
5312				HR	North	HR-6	44.668842	125.108615	615	NatPine
5097			Low Act.	HR	North	HR-4	44.670075	125.098674	595	DougFir
5126				HR	North	HR-8	44.667636	125.100737	601	DougFir
5211				HR	North	HR-5	44.669562	125.103934	618	DougFir
5304				HR	South	HR-2	44.570284	125.152849	810	DougFir
5361				HR	South	HR-12	44.568043	125.153013	792	DougFir
5364				HR	South	HR-10	44.568151	125.153038	788	DougFir
5095				HR	North	HR-4	44.670075	125.098674	595	NatFir
5192				HR	North	HR-8	44.667636	125.100700	604	NatFir
5309				HR	North	HR-5	44.669562	125.103934	618	NatFir
5363				HR	South	HR-10	44.568151	125.153038	788	NatFir
5096				HR	North	HR-4	44.670084	125.098674	595	NatPine
5191				HR	North	HR-8	44.667636	125.100700	604	NatPine
5310				HR	North	HR-5	44.669562	125.103934	618	NatPine

[a]HR=Hydrate Ridge; CR=Costa Rica; ERB=Eel River Basin

[b]These native samples also served as controls for the transplantation expereiments (see main text).

[c]For transplant experiment samples, the seepage activity at their final deployment location is listed.

[d]A=aragonite; AC=aragonite/calcite mixture; C=calcite, CD=calcite/dolomite mixture; D=dolomite; ACD=aragonte/calcite/dolomite mixture.

[e]Sediment and nodule samples previously examined in Mason et al., 2015.

Throughout table, n.a. indicates "not applicable" and n.m. indicates "not measured"

Supplementary Table 2. List of ANOSIM tests. Significance values (p-values) are colored green if <0.05 and red if >0.05.

Environmental Variable Tested	Sample Set	R	p
Habitat Substrate	Native sediments, nodules, carbonates, and bottom water	0.49	0.001
Activity		0.29	0.001
Habitat Substrate	Sediments and nodules	0.09	0.098
Habitat Substrate	Sediments and nodules (binned as one group) and native carbonates	0.49	0.001
Regional Geography	Sediments and nodules	0.51	0.001
Activity		0.43	0.009
Treatment	Transplant controls and native carbonates	-0.01	0.521
Activity	Native carbonates	0.45	0.001
1000s of km biogeography (Costa Rica *vs* Hydrate Ridge)		-0.05	0.713
Mineralogy		0.44	0.001
Mineralogy	Native, active carbonates	0.45	0.001
Mineralogy	Native, low activity carbonates	0.30	0.041
10s of km biogeography (HR-North *vs* HR-South *vs* SE-Knoll)	Native carbonates at Hydrate Ridge (excluding Costa Rica)	-0.06	0.788
Activity		0.50	0.001
Cruise Collected		-0.02	0.652
Specific Collection Site (e.g. HR-3)	Native, active carbonates at Hydrate Ridge (excluding Costa Rica)	0.31	0.002
Specific Collection Site (e.g. HR-4)	Native, low activity carbonates at Hydrate Ridge (excluding Costa Rica)	0.27	0.037
Experimental Treatment	Native and transplanted carbonates	0.49	0.001
Experimental Treatment	Native, active carbonates and transplant-to-low activity carbonates	0.32	0.008
Experimental Treatment	Native, low activity carbonates and transplant-to-low activity carbonates	0.88	0.001
Experimental Treatment	Native sediments, nodules, carbonates, and bottom water (binned as one group) and colonization carbonates and woods (binned as one group)	0.68	0.001
Experimental Treatment	Native carbonates and colonization carbonates	0.65	0.001
Experimental Treatment	Native carbonates and colonizatoin carbonates (Presence/Absence normalized)	0.53	0.001
Habitat Substrate	Colonization carbonates and woods	0.63	0.001
Activity		0.38	0.001
Activity	Colonization carbonates	0.81	0.001
Mineralogy		0.11	0.109
Activity	Colonization woods	0.39	0.001
Wood Type		0.22	0.008
Wood Type	Colonization woods, active	0.12	0.203
Wood Type	Colonization woods, low activity	0.56	0.002

Supplementary Table 3. Relative abundance information is listed for OTUs presented in Fig. 3, Fig. 4, and Fig. 5 of the main text, for all 134 samples in this study. Data is provided in four tabs: (Tab 1) Raw data associated with Fig. 3; (Tab 2) Raw data associated with Fig. 4G; (Tab 3) Raw data associated with Fig. 4H; (Tab 4) Raw data ssociated with Fig. 5. For the data used to generate Fig. 5, in all cases a minority of the OTUs were identified for presentation (e.g., 3 of 8 for ANME-1). However, these represented the majority of the total sequences recovered among each taxonomy (e.g., 95% of all sequences for ANME-1). Bold boxes outline the sets of OTUs which were binned for presentation in Fig. 5. Colors scales are meant to aid the reader in assessing OTU distribution. OTUs of the same phylogeny were combined for presentation in Fig. 5 of the main text.

Supplementary Table 3 can be found in .xlsx format in the Caltech online repository along with this thesis.

2.10 SUPPLEMENTAL MATERIAL: FIGURES

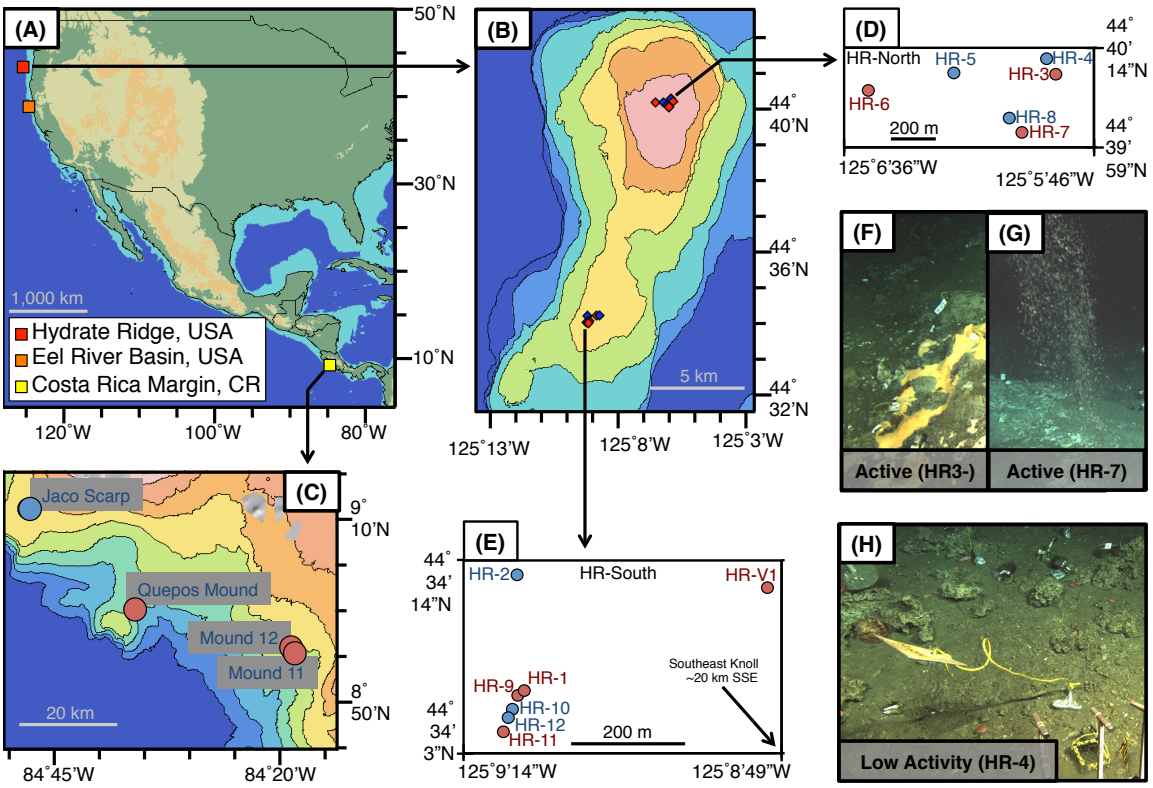

Supplementary Figure 1. Overview map of sampling locations in this study. For seep descriptions, see Section 2.1. (A) Overview the three seep locations sampled in this study, (B) map of Hydrate Ridge including sampling locations at HR-North and HR-South, (C) map of Costa Rica including the four mounds sampled for native carbonates, (D) map of HR-North showing spatial relationship between stations HR-3, -4, -5, -6, -7, and -8, (E) map of HR-South showing spatial relationship between stations HR-1, -2, -9, -10, -11, -12, and -V1, (F-G) seafloor images of active stations HR-3 and HR-7 exhibiting orange bacterial mats (HR-3), clam beds (HR-3 & HR-7), and methane ebullition (HR-7), (H) seafloor image of low-activity station HR-4 lacking the diagnostic indicators seen in (F-G). Subplots (A-C) generated in GeoMapApp (http://www.geomapapp.org, [Ryan et al., 2009]). For subplot (B), contour lines represent 100 m bathymetric relief with HR-North the shallowest at 700 mbsl. For subplot (C), contour lines represent 250 m bathymetric relief with the shallow continental shelf at 250 mbsl in the NE corner. Red and blue points plotted in subplots (B-E) represent active and low-activity stations, respectively.

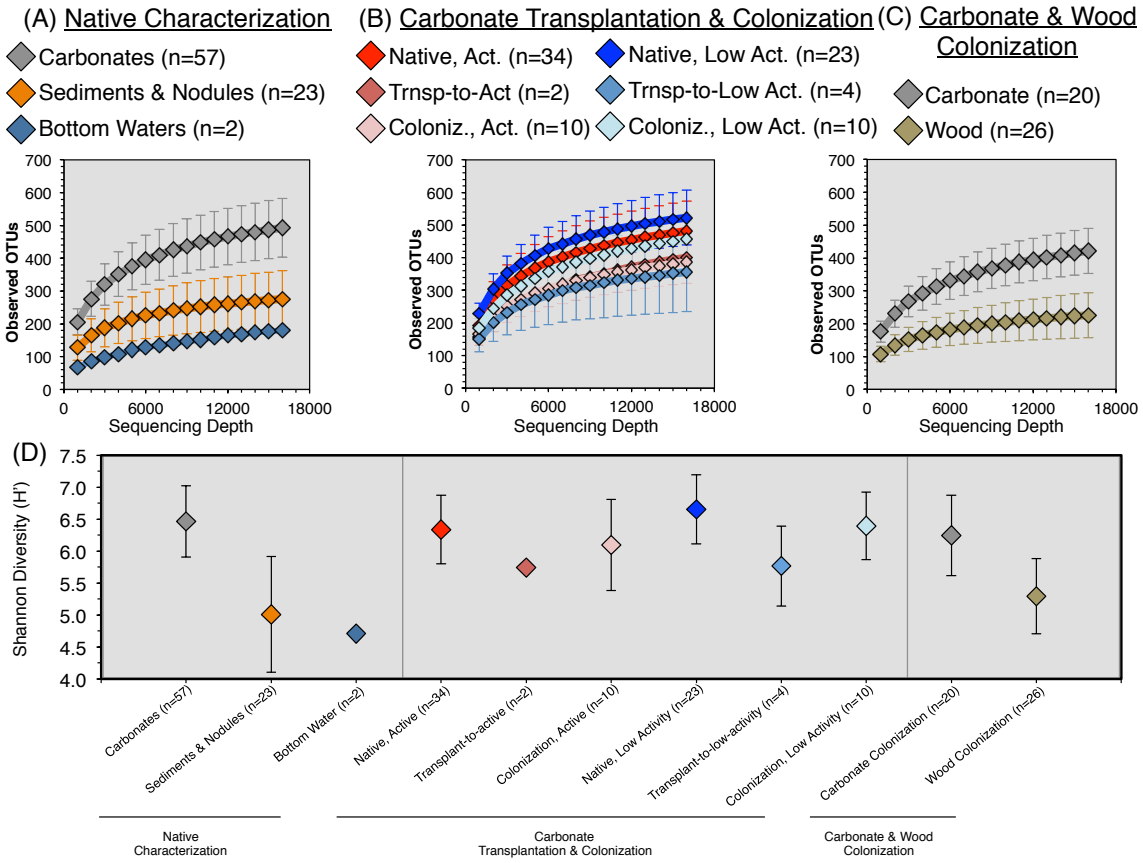

Supplementary Figure 2. Additional alpha diversity metrics for the samples in this study. (A-C) Collector's curves of raw OTU_{97}, for the native samples (A), carbonate samples (B), and colonization samples (C). (D) Shannon Diversity (H') for the major sample groups analyzed in this study. Error bars represent standard deviation among the sample groups, which is not included for the bottom water and transplant-to-active samples due to the low number of replicates.

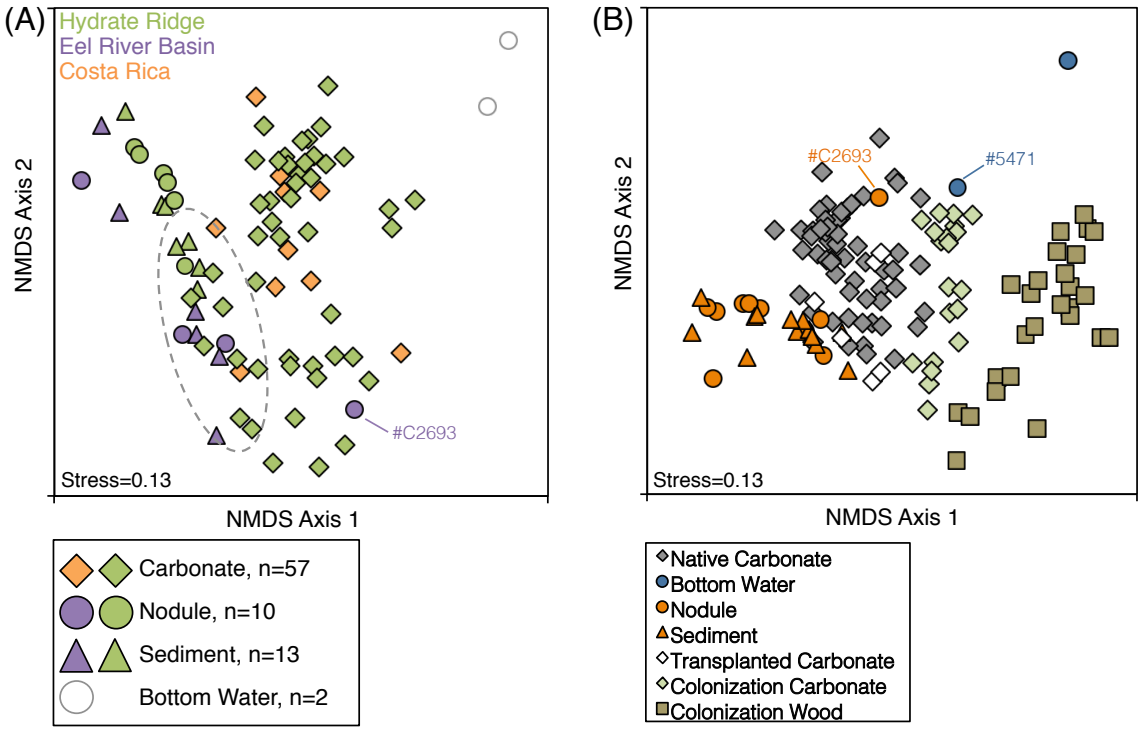

Supplementary Figure 3. Additional non-metric multidimensional scaling analyses (A) Ordination of the sample data from native carbonates, sediments, nodules, and bottom water. Ordination is identical to Fig. 1A, but the carbonates, sediments, and nodules are colored by geographic origin. The overlap between Costa Rica and Hydrate Ridge carbonates, in the same vicinity on the plot as Hydrate Ridge and Eel River Basin sediments and nodules, demonstrates that the region where habitat substrates overlap (roughly, the dashed circle) is not a geographic effect. (B) All 134 samples in this study. The same intra-sample relationships are visible as in Fig. 1. The wood colonization samples plot in a distinct region away from all other samples, though most similar to the colonization carbonates. Sample #C2693 is highlighted as a biological outlier among the nodule-hosted samples. Sample #5471 is highlighted because in this ordination plot of all samples, it appears biologically similar to some of the carbonate colonization samples. Sample #5471 was bottom water from an active seep site (Table S1), which may be related to its similarity to some colonization samples; more bottom water data points would be necessary in order to draw a stronger conclusion.

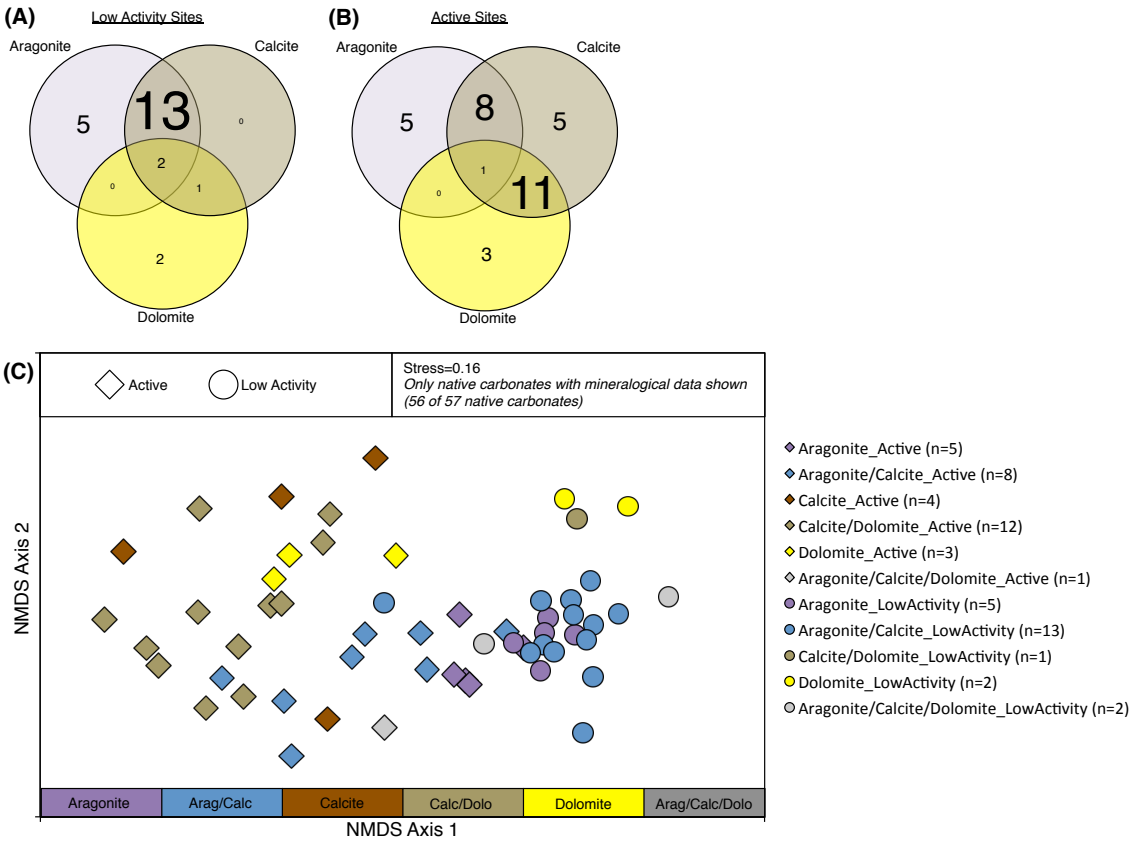

Supplementary Figure 4. Mineralogical Analysis. (A-B) Distribution of recovered carbonate mineralogies at low-activity (A) and active seep stations (B). Note that aragonite-bearing mineralogies are dominant at low-activity stations, while active seep stations host more varied mineralogies including a greater proportion of dolomite-bearing carbonates. In order to emphasize the distributions, text size is proportional to value. From this data, it appears that carbonate mineralogy may have a loose correlation with seep activity. From our dataset we are unable to determine whether mineralogy and seep activity are truly dependent or independent environmental variables (see Supplemental Text). (C) Non-metric multidimensional scaling analysis of microbial assemblages from native carbonate samples according to seep activity and mineralogy. Samples are separated according to seep activity (c.f. Fig. 1B), but such a difference is also qualitatively correlated with mineralogical differences.

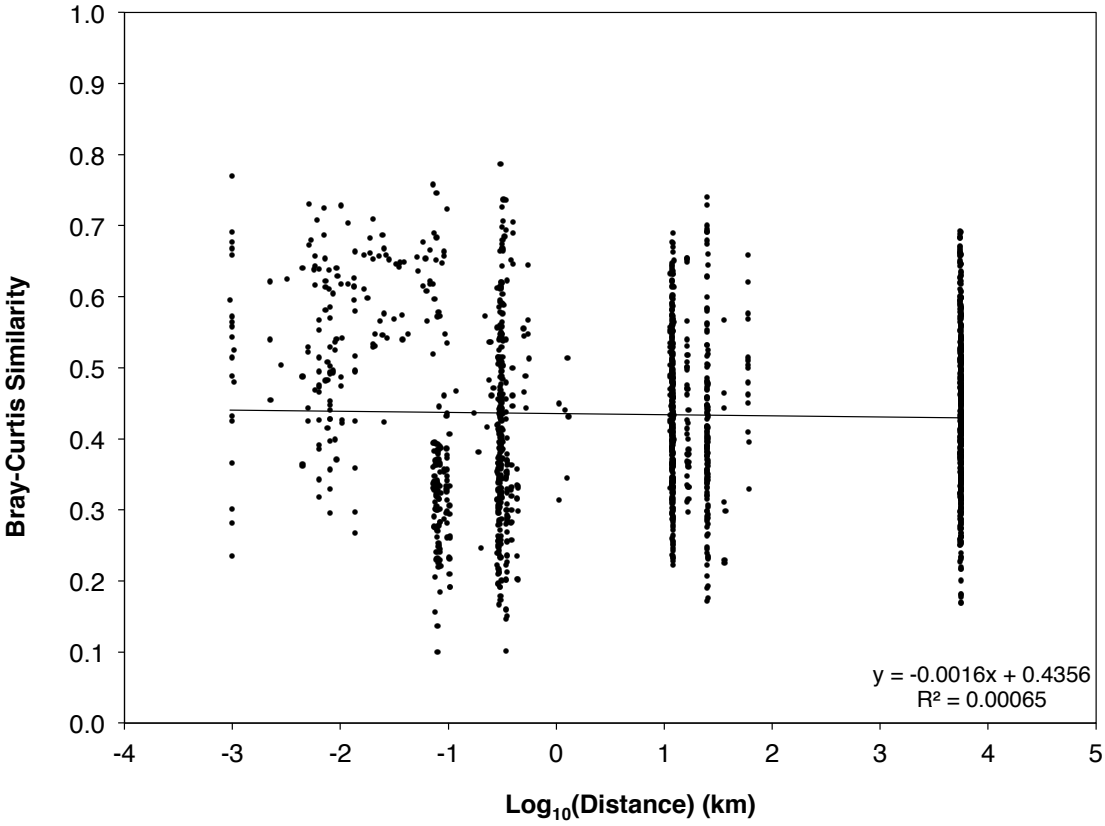

Supplementary Figure 5. Distance-decay plot of the 57 native carbonates collected from Hydrate Ridge and Costa Rica. Geographical distance is calculated in km along a Great Circle between each sample pair (R package 'geosphere' v1.3-13, function 'distHaversine', assuming a spherical Earth of radius of 6,371 km). Bray-Curtis similarity is calculated as described in the main text, presented with a value of '1' being identical similarity, and '0' being complete dissimilarity. Note the y-axis is linear and the x-axis is logarithmic. No correlation is observed between Bray-Curtis similarity and geographic distance. Although this does not preclude such a correlation existing, it means that such a correlation may be aliased by influences of other environmental factors (e.g., seep activity).

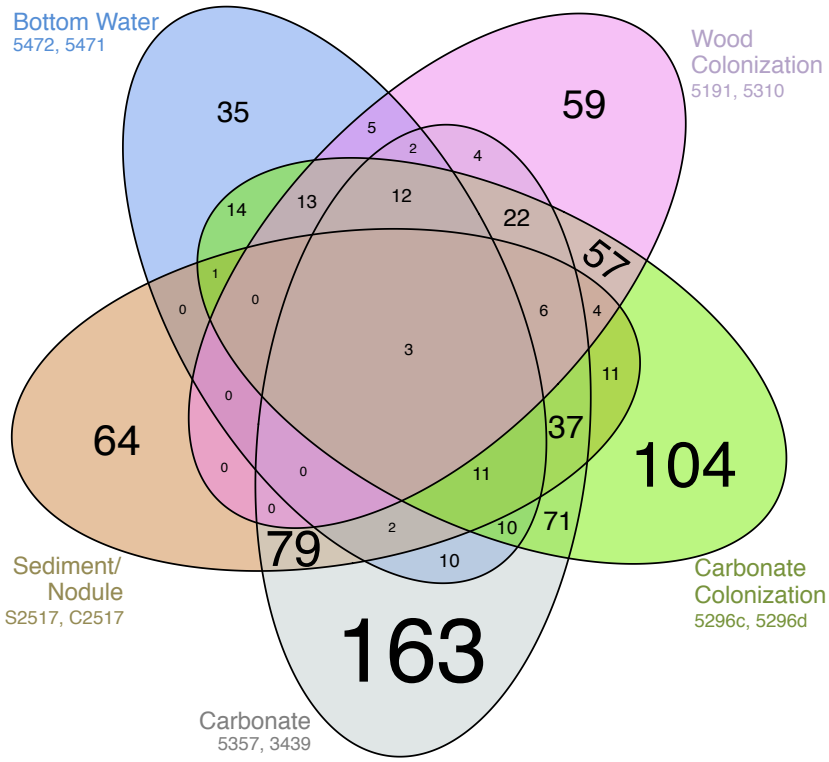

Supplementary Figure 6. OTU overlap between colonized substrates at active site HR-9, including representative native substrates. Site HR-9 was chosen because it was the associated site for both bottom water samples, it hosted both carbonate and wood colonization experiments, it hosted multiple native carbonates which were recovered and analyzed, and it was an active seep site. Since sediment and nodule samples were not collected from HR-9, representatives of those substrates were chosen from another HR-South location (HR-V1); shallow (0-3 cmbsf) sediments and nodules were chosen because they were most likely to be relevant for colonization experiments which were performed on the seafloor. In order to keep the Venn diagram relatively simple, and because ANOSIM tests revealed sediments and nodules to be indistinguishable from one another, sediments and nodules were binned together as one “habitat type” for this analysis. In order to ensure equal depth of sampling across each substrate type, two representative samples of each substrate were chosen randomly (see sample numbers on the Figure). In order to emphasize the distributions, text size is proportional to OTU occurrence. For all OTU overlap diagrams, the specific samples analyzed are given in small text next to the diagram bubbles. In order for an OTU to be counted as “present” for a category (e.g., for an OTU to be associated with “Bottom Water”), it had to be present in *both* replicates. This approach ensured that the OTUs under examination were reproducibly recovered from every category, rather than spurious observations.

2.11 REFERENCES

Alain, K., M. Zbinden, N. Le Bris, F. Lesongeur, J. Quérellou, F. Gaill, and M. A. Cambon Bonavita. 2004. Early steps in microbial colonization processes at deep-sea hydrothermal vents. Environmental microbiology **6**: 227–241.

Bekins, B. A., and S. J. Dreiss. 1992. A simplified analysis of parameters controlling dewatering in accretionary prisms. Earth and Planetary Science Letters **109**: 275–287.

Bernard, C., and T. Fenchel. 1995. Mats of colourless sulphur bacteria. II. Structure, composition of biota and successional patterns. Marine Ecology Progress Series **128**: 171–179.

Bian, Y., D. Feng, H. H. Roberts, and D. Chen. 2013. Tracing the evolution of seep fluids from authigenic carbonates: Green Canyon, northern Gulf of Mexico. Marine and Petroleum Geology **44**: 71–81.

Bienhold, C., P. Pop Ristova, F. Wenzhöfer, T. Dittmar, and A. Boetius. 2013. How Deep-Sea Wood Falls Sustain Chemosynthetic Life. PLoS ONE **8**: e53590.

Birgel, D., T. Himmler, A. Freiwald, and J. Peckmann. 2008. A new constraint on the antiquity of anaerobic oxidation of methane: Late Pennsylvanian seep limestones from southern Namibia. Geology **36**: 543–546.

Blumenberg, M., E.-O. Walliser, M. Taviani, R. Seifert, and J. Reitner. 2015. Authigenic carbonate formation and its impact on the biomarker inventory at hydrocarbon seeps – a case study from the Holocene Black Sea and the Plio-Pleistocene Northern Apennines (Italy). Marine and Petroleum Geology **66**: 532–541.

Boetius, A., and E. Suess. 2004. Hydrate Ridge: a natural laboratory for the study of microbial life fueled by methane from near-surface gas hydrates. Chemical Geology **205**: 291–310.

Boetius, A., K. Ravenschlag, C. J. Schubert, D. Rickert, F. Widdel, A. Gieseke, R. Amann, B. B. Jørgensen, U. Witte, and O. Pfannkuche. 2000. A marine microbial consortium apparently mediating anaerobic oxidation of methane. Nature **407**: 623–626.

Bowman, J. P., and R. D. McCuaig. 2003. Biodiversity, Community Structural Shifts, and Biogeography of Prokaryotes within Antarctic Continental Shelf Sediment. Applied and Environmental Microbiology **69**: 2463–2483.

Caporaso, J. G., C. L. Lauber, W. A. Walters, D. Berg-Lyons, C. A. Lozupone, P. J. Turnbaugh, N. Fierer, and R. Knight. 2011. Global patterns of 16S rRNA diversity at a depth of millions of sequences per sample. Proceedings of the National Academy of Sciences **108**: 4516–4522.

Caporaso, J. G., C. L. Lauber, W. A. Walters, D. Berg-Lyons, J. Huntley, N. Fierer, S. M. Owens, J. Betley, L. Fraser, M. Bauer, N. Gormley, J. A. Gilbert, G. Smith, and R. Knight. 2012. Ultra-high-throughput microbial community analysis on the Illumina HiSeq and MiSeq platforms. The ISME Journal **6**: 1621–1624.

Chen, Z., W. Yan, M. Chen, S. Wang, J. Lu, F. Zhang, R. Xiang, S. Xiao, P. Yan, and S. Gu. 2006. Discovery of seep carbonate nodules as new evidence for gas venting on the northern continental slope of South China Sea. Chinese Science Bulletin **51**: 1228–1237.

Clarke, K. R., and R. M. Warwick. 2001. Change in Marine Communities, 2nd ed. PRIMER-E Ltd.

Dekas, A. E., G. L. Chadwick, M. W. Bowles, S. B. Joye, and V. J. Orphan. 2014. Spatial distribution of nitrogen fixation in methane seep sediment and the role of the ANME archaea. Environmental microbiology **16**: 3012–3029.

Distel, D. L., A. R. Baco, E. Chuang, W. Morrill, C. Cavanaugh, and C. R. Smith. 2000. Marine ecology: Do mussels take wooden steps to deep-sea vents? Nature **403**: 725–726.

Fagervold, S. K., C. Romano, D. Kalenitchenko, C. Borowski, A. Nunes-Jorge, D. Martin, and P. E. Galand. 2014. Microbial Communities in Sunken Wood Are Structured by Wood-Boring Bivalves and Location in a Submarine Canyon D.A. Carter [ed.]. PLoS ONE **9**: e96248.

Fagervold, S. K., P. E. Galand, M. Zbinden, F. Gaill, P. Lebaron, and C. Palacios. 2012. Sunken

woods on the ocean floor provide diverse specialized habitats for microorganisms. FEMS Microbiology Ecology **82**: 616–628.

Garrity, G. M., D. J. Brenner, N. R. Krieg, and J. T. Staley, eds. 2005. Bergey's Manual of Systematic Bacteriology, Volume Two: The Proteobacteria, Springer.

Gieskes, J., C. Mahn, S. Day, J. Martin, J. Greinert, T. Rathburn, and B. McAdoo. 2005. A study of the chemistry of pore fluids and authigenic carbonates in methane seep environments: Kodiak Trench, Hydrate Ridge, Monterey Bay, and Eel River Basin. Chemical Geology **220**: 329–345.

Gilbert, J. A., F. Meyer, J. Jansson, J. Gordon, N. R. Pace, J. M. Tiedje, R. E. Ley, N. Fierer, D. Field, N. C. Kyrpides, F. O. Gloeckner, H. P. Klenk, K. E. Wommack, E. Glass, K. Docherty, R. Gallery, R. Stevens, and R. Knight. 2011. The Earth Microbiome Project: Meeting report of the "1st EMP meeting on sample selection and acquisition" at Argonne National Laboratory October 6th 2010. 1–5.

Girguis, P., V. Orphan, S. Hallam, and E. F. DeLong. 2003. Growth and methane oxidation rates of anaerobic methanotrophic archaea in a continuous-flow bioreactor. Applied and Environmental Microbiology **69**: 5472–5482.

Green-Saxena, A., A. E. Dekas, N. F. Dalleska, and V. J. Orphan. 2014. Nitrate-based niche differentiation by distinct sulfate-reducing bacteria involved in the anaerobic oxidation of methane. The ISME Journal **8**: 150–163.

Greinert, J., G. Bohrmann, and E. Suess. 2001. Gas Hydrate-Associated Carbonates and Methane-Venting at Hydrate Ridge: Classification, Distribution, and Origin of Authigenic Lithologies, p. 99–113. *In* C.K. Paull and W.P. Dillon [eds.], Natural Gas Hydrates. American Geophysical Union.

Guilini, K., L. A. Levin, and A. Vanreusel. 2012. Cold seep and oxygen minimum zone associated sources of margin heterogeneity affect benthic assemblages, diversity and nutrition at the Cascadian margin (NE Pacific Ocean). Progress in Oceanography **96**: 77–92.

Heijs, S. K., G. Aloisi, I. Bouloubassi, R. D. Pancost, C. Pierre, J. S. Sinninghe Damsté, J. C. Gottschal, J. D. Elsas, and L. J. Forney. 2006. Microbial Community Structure in Three Deep-Sea Carbonate Crusts. Microbial Ecology **52**: 451–462.

Hinrichs, J. M. Hayes, S. P. Sylva, P. G. Brewer, and E. F. DeLong. 1999. Methane-consuming archaebacteria in marine sediments. Nature **398**: 802–805.

Hovland, M., M. R. Talbot, H. Qvale, S. Olaussen, and L. Aasberg. 1987. Methane-related Carbonate Cements in Pockmarks of the North Sea. Journal of Sedimentary Petrology **57**: 881–892.

Ijiri, A., U. Tsunogai, T. Gamo, F. Nakagawa, T. Sakamoto, and S. Saito. 2009a. Enrichment of adsorbed methane in authigenic carbonate concretions of the Japan Trench. Geo-Marine Letters **29**: 301–308.

Knittel, K., T. Lösekann, A. Boetius, R. Kort, and R. Amann. 2005. Diversity and Distribution of Methanotrophic Archaea at Cold Seeps. Applied and Environmental Microbiology **71**: 467–479.

Kontoyannis, C. G., and N. V. Vagenas. 2000. Calcium carbonate phase analysis using XRD and FT-Raman spectroscopy. The Analyst **125**: 251-255.

Krause, S., V. Liebetrau, S. Gorb, M. Sanchez-Roman, J. A. McKenzie, and T. Treude. 2012. Microbial nucleation of Mg-rich dolomite in exopolymeric substances under anoxic modern seawater salinity: New insight into an old enigma. Geology **40**: 587–590.

Levin, L. A. 2005. Ecology of cold seep sediments: Interactions of fauna with flow, chemistry, and microbes. Oceanography and Marine Biology: An Annual Review **43**: 1–46.

Levin, L. A., G. F. Mendoza, B. M. Grupe, J. P. Gonzalez, B. Jellison, G. W. Rouse, A. R. Thurber, and A. Waren. 2015. Biodiversity on the Rocks: Macrofauna Inhabiting Authigenic Carbonate at Costa Rica Methane Seeps. PLoS ONE 1–31.

Levin, L. A., G. F. Mendoza, J. P. Gonzalez, A. R. Thurber, and E. E. Cordes. 2010. Diversity of

bathyal macrofauna on the northeastern Pacific margin: the influence of methane seeps and oxygen minimum zones. Marine Ecology Progress Series **31**: 94–110.

Levin, L. A., V. J. Orphan, G. W. Rouse, A. E. Rathburn, W. Ussler, G. S. Cook, S. K. Goffredi, E. M. Perez, A. Waren, B. M. Grupe, G. Chadwick, and B. Strickrott. 2012. A hydrothermal seep on the Costa Rica margin: middle ground in a continuum of reducing ecosystems. Proceedings of the Royal Society of London B 1–9.

Levin, L. A., W. Ziebis, G. F. Mendoza, V. Growney, M. D. Tryon, K. M. Brown, C. Mahn, J. M. Gieskes, and A. E. Rathburn. 2003. Spatial heterogeneity of macrofauna at northern California methane seeps: influence of sulfide concentration and fluid flow. Marine Ecology Progress Series **265**: 123–139.

Li, L., C. Kato, and K. Horikoshi. 1999. Microbial Diversity in Sediments Collected from the Deepest Cold-Seep Area, the Japan Trench. Marine Biotechnology **1**: 391–400.

Marlow, J. J., J. A. Steele, W. Ziebis, A. R. Thurber, L. A. Levin, and V. J. Orphan. 2014a. Carbonate-hosted methanotrophy represents an unrecognized methane sink in the deep sea. Nature Communications **5**: 1–12.

Marlow, J., J. A. Steele, D. Case, S. A. Connon, L. A. Levin, and V. J. Orphan. 2014b. Microbial abundance and diversity patterns associated with sediments and carbonates from the methane seep environments of Hydrate Ridge, OR. Frontiers in Marine Science **1**: 1–16.

Marlow, J., J. Peckmann, and V. Orphan. 2015. Autoendoliths: a distinct type of rock-hosted microbial life. Geobiology **13**: 303–307.

Mason, O. U., D. H. Case, T. H. Naehr, R. W. Lee, R. B. Thomas, J. V. Bailey, and V. J. Orphan. 2015. Comparison of Archaeal and Bacterial Diversity in Methane Seep Carbonate Nodules and Host Sediments, Eel River Basin and Hydrate Ridge, USA. Microbial Ecology **70**: 776–784.

Morono, Y., T. Terada, M. Nishizawa, M. Ito, F. Hillion, N. Takahata, Y. Sano, and F. Inagaki. 2011. Carbon and nitrogen assimilation in deep subseafloor microbial cells. Sci. Dril. **108**: 18295–18300.

Naehr, T. H., P. Eichhubl, V. J. Orphan, M. Hovland, C. K. Paull, W. Ussler, T. D. Lorenson, and H. G. Greene. 2007. Authigenic carbonate formation at hydrocarbon seeps in continental margin sediments: a comparative study. Deep Sea Research Part II **54**: 1268–1291.

Niemann, H., P. Linke, K. Knittel, E. MacPherson, A. Boetius, W. Brückmann, G. Larvik, K. Wallmann, U. Schacht, E. Omoregie, D. Hilton, K. Brown, and G. Rehder. 2013. Methane-Carbon Flow into the Benthic Food Web at Cold Seeps – A Case Study from the Costa Rica Subduction Zone. PLoS ONE **8**: e74894.

Nunoura, T., Y. Takaki, H. Kazama, M. Hirai, J. Ashi, H. Imachi, and K. Takai. 2012. Microbial Diversity in Deep-sea Methane Seep Sediments Presented by SSU rRNA Gene Tag Sequencing. Microbes and Environments **27**: 382–390.

Orphan, V. J., Hinrichs, W. Ussler, C. K. Paull, L. T. Taylor, S. P. Sylva, J. M. Hayes, and E. F. Delong. 2001. Comparative Analysis of Methane-Oxidizing Archaea and Sulfate-Reducing Bacteria in Anoxic Marine Sediments. Applied and Environmental Microbiology **67**: 1922–1934.

Orphan, V. J., K. A. Turk, A. M. Green, and C. H. House. 2009. Patterns of 15N assimilation and growth of methanotrophic ANME-2 archaea and sulfate-reducing bacteria within structured syntrophic consortia revealed by FISH-SIMS. Environmental microbiology **11**: 1777–1791.

Orphan, V., W. Ussler, T. H. Naehr, C. H. House, Hinrichs, and C. K. Paull. 2004. Geological, geochemical, and microbiological heterogeneity of the seafloor around methane vents in the Eel River Basin, offshore California. Chemical Geology **205**: 265–289.

Peckmann, J., A. Reimer, C. Luth, C. Luth, B. T. Hansen, C. Heinicke, J. Hoefs, and J. Reitner. 2001. Methane-derived carbonates and authigenic pyrite from the northwestern Black Sea.

Marine Geology **177**: 129–150.

Pop Ristova, P., F. Wenzhöfer, A. Ramette, J. Felden, and A. Boetius. 2015. Spatial scales of bacterial community diversity at cold seeps (Eastern Mediterranean Sea). The ISME Journal **9**: 1306–1318.

R Core Team. 2014. R: A language and environment for statistical computing.

Rajala, P., M. Bomberg, R. Kietäväinen, I. Kukkonen, L. Ahonen, M. Nyyssönen, and M. Itävaara. 2015. Rapid Reactivation of Deep Subsurface Microbes in the Presence of C-1 Compounds. Microorganisms **3**: 17–33.

Reitner, J., J. Peckmann, A. Reimer, G. Schumann, and V. Thiel. 2005. Methane-derived carbonate build-ups and associated microbial communities at cold seeps on the lower Crimean shelf (Black Sea). Facies **51**: 66–79.

Rossel, P. E., M. Elvert, A. Rammette, A. Boetius, and Hinrichs. 2011. Factors controlling the distribution of anaerobic methanotrophic communities in marine environments: Evidence from intact polar membrane lipids. Geochimica et Cosmochimica Acta **75**: 164–184.

Ruff, S. E., J. Arnds, K. Knittel, R. Amann, G. Wegener, A. Ramette, and A. Boetius. 2013. Microbial Communities of Deep-Sea Methane Seeps at Hikurangi Continental Margin (New Zealand). PLoS ONE **8**: e72627.

Ruff, S. E., J. F. Biddle, A. P. Teske, K. Knittel, A. Boetius, and A. Ramette. 2015. Global dispersion and local diversification of the methane seep microbiome. Proceedings of the National Academy of Sciences 1–6.

Ryan, W. B. F., S. M. Carbotte, J. O. Coplan, S. O'Hara, A. Melkonian, R. Arko, R. A. Weissel, V. Ferrini, A. Goodwillie, F. Nitsche, J. Bonczkowski, and R. Zemsky. 2009. Global Multi-Resolution Topography synthesis. Geochemistry Geophysics Geosystems **10**: 1-9.

Sahling, H., D. G. Masson, C. R. Ranero, V. Hühnerbach, W. Weinrebe, I. Klaucke, D. Bürk, W. Brückmann, and E. Suess. 2008. Fluid seepage at the continental margin offshore Costa Rica and southern Nicaragua. Geochemistry Geophysics Geosystems **9**: 1–22.

Sahling, H., D. Rickert, R. W. Lee, P. Linke, and E. Suess. 2002. Macrofaunal community structure and sulfide flux at gas hydrate deposits from the Cascadia convergent margin, NE Pacific. Marine Ecology Progress Series **231**: 121–138.

Schauer, R., C. Bienhold, A. Ramette, and J. Harder. 2010. Bacterial diversity and biogeography in deep-sea surface sediments of the South Atlantic Ocean. The ISME Journal **4**: 159–170.

Schmale, O., I. Leifer, J. Schneider von Deimling, C. Stolle, S. Krause, K. Kießlich, A. Fram, and T. Treude. 2015. Bubble transport mechanism: Indications for a gas bubble-mediated inoculation of benthic methanothrophs into the water column. Continental Shelf Research **103**: 70–78.

Sievert, S. M., E. B. A. Wieringa, C. O. Wirsen, and C. D. Taylor. 2007. Growth and mechanism of filamentous-sulfur formation by Candidatus Arcobacter sulfidicus in opposing oxygen-sulfide gradients. Environmental microbiology **9**: 271–276.

Sorokin, D. Y., T. P. Tourova, E. Y. Bezsoudnova, A. Pol, and G. Muyzer. 2007. Denitrification in a binary culture and thiocyanate metabolism in Thiohalophilus thiocyanoxidans gen. nov. sp. nov. – a moderately halophilic chemolithoautotrophic sulfur-oxidizing Gammaproteobacterium from hypersaline lakes. Archives of microbiology **187**: 441–450.

Stadnitskaia, A., G. Muyzer, B. Abbas, M. J. L. Coolen, E. C. Hopmans, M. Baas, T. C. E. van Weering, M. K. Ivanov, E. Poludetkina, and J. S. Sinninghe Damsté. 2005. Biomarker and 16S rDNA evidence for anaerobic oxidation of methane and related carbonate precipitation in deep-sea mud volcanoes of the Sorokin Trough, Black Sea. Marine Geology **217**: 67–96.

Suess, E., B. Carson, S. D. Ritger, J. C. Moore, M. L. Jones, L. D. Kulm, and G. R. Cochrane. 1985. Biological communities at vent sites along the subduction zone off Oregon. Bulletin of the Biological Society of Washington **6**: 475–484.

Sylvan, J. B., B. C. Pyenson, O. Rouxel, C. R. German, and K. J. Edwards. 2012a. Time-series analysis of two hydrothermal plumes at 9°50′N East Pacific Rise reveals distinct,

heterogeneous bacterial populations. Geobiology **10**: 178–192.

Sylvan, J. B., B. M. Toner, and K. J. Edwards. 2012b. Life and Death of Deep-Sea Vents: Bacterial Diversity and Ecosystem Succession on Inactive Hydrothermal Sulfides. mBio **3**: e00279–11.

Tavormina, P., W. Ussler, S. Joye, B. Harrison, and V. Orphan. 2010. Distributions of putative aerobic methanotrophs in diverse pelagic marine environments. The ISME Journal **4**: 700–710.

Taylor, C. D., C. O. Wirsen, and F. Gaill. 1999. Rapid Microbial Production of Filamentous Sulfur Mats at Hydrothermal Vents. Applied and Environmental Microbiology **65**: 2253–2255.

Teichert, B., G. Bohrmann, and E. Suess. 2005. Chemoherms on Hydrate Ridge--Unique microbially-mediated carbonate build-ups growing into the water column. Palaeogeography, Palaeoclimatology, Palaeoecology **227**: 67–85.

Thiel, V., J. Peckmann, H. H. Richnow, U. Luth, J. Reitner, and W. Michaelis. 2001. Molecular signals for anaerobic methane oxidation in Black Sea seep carbonates and a microbial mat. Marine Chemistry **73**: 97–112.

Thurber, A. R., L. A. Levin, V. J. Orphan, and J. J. Marlow. 2012. Archaea in metazoan diets: implications for food webs and biogeochemical cycling. The ISME Journal **6**: 1602–1612.

Trembath-Reichert, E., D. H. Case, and V. J. Orphan. 2016. Characterization of microbial associations with methanotrophic archaea and sulfate-reducing bacteria through statistical comparison of nested Magneto-FISH enrichments. PeerJ **4**: 31913-31.

Treude, T., A. Boetius, K. Knittel, K. Wallmann, and B. B. Jørgensen. 2003. Anaerobic oxidation of methane above gas hydrates at Hydrate Ridge, NE Pacific Ocean. Marine Ecology Progress Series **264**: 1–14.

Tryon, M. D., K. M. Brown, and M. E. Torres. 2002. Fluid and chemical flux in and out of sediments hosting methane hydrate deposits on Hydrate Ridge, OR, II: Hydrological processes. Earth and Planetary Science Letters **201**: 541–557.

Tryon, M. D., K. M. Brown, M. E. Torres, A. M. Tréhu, J. McManus, and R. W. Collier. 1999. Measurements of transience and downward fluid flow near episodic methane gas vents, Hydrate Ridge, Cascadia. Geology **27**: 1075–1078.

Watanabe, Y., S. Nakai, A. Hiruta, R. Matsumoto, and K. Yoshida. 2008. U–Th dating of carbonate nodules from methane seeps off Joetsu, Eastern Margin of Japan Sea. Earth and Planetary Science Letters **272**: 89–96.

Zhang, F., H. Xu, H. Konishi, and E. E. Roden. 2010. A relationship between d104 value and composition in the calcite-disordered dolomite solid-solution series. American Mineralogist **95**: 1650-1656.